Eindhoven University of Technology

BACHELOR

Data collection for suction cup modelling at varying internal pressure

Hage, Max L.

Award date:
2023

Link to publication

Disclaimer
This document contains a student thesis (bachelor's or master's), as authored by a student at Eindhoven University of Technology. Student theses are made available in the TU/e repository upon obtaining the required degree. The grade received is not published on the document as presented in the repository. The required complexity or quality of research of student theses may vary by program, and the required minimum study period may vary in duration.

General rights
Copyright and moral rights for the publications made accessible in the public portal are retained by the authors and/or other copyright owners and it is a condition of accessing publications that users recognise and abide by the legal requirements associated with these rights.

- Users may download and print one copy of any publication from the public portal for the purpose of private study or research.
- You may not further distribute the material or use it for any profit-making activity or commercial gain

EINDHOVEN UNIVERSITY OF TECHNOLOGY

Department of Mechanical Engineering
Dynamics and Control Section

Data collection for suction cup modelling at varying internal pressure

Bachelor End Project
DC 2023.012

M.L. Hage
1246704

Project supervisors:
Dr. ir. Alessandro Saccon
Dr. Alexander Oliva

Eindhoven, January 21, 2023

List of symbols

Symbol	Definition	Unit
A	Body-fixed frame located at the tip of the tool arm	
P	Body-fixed frame located at centre of the VIO plate	
F_g	Gravitational force	N
F_{spring}	Force exerted by a spring (i.e. the suction cup)	N
g	Gravitational acceleration	m/s
I	Area moment of inertia	m^4
k	spring constant	N/m
$\hat{k}$	estimated spring constant	N/m
l	Length	m
m	Mass	kg
M_{max}	maximum load applied on the VIO plate	g
P_{inflow}	air supply inflow pressure	bar
$P_{internal}$	suction cup internal pressure	bar
P_{volt}	pressure sensor output	volt
x	spring elongation	m
$\hat{x}$	estimated spring elongation	mm
x_{mean}	mean measured elongation	mm
V	Volume	m^3

Contents

1 Introduction

In this chapter the research project is introduced by presenting background information and motivation. The research goal of the project will be discussed as well as the report structure.

1.1 Background information and motivation

The worldwide e-commerce market has grown steadily in recent years and is predicted to keep on growing. E-commerce, short for electronic commerce, refers to the buying and selling of goods and services through internet. According to a recent industry report, e-commerce accounts for 20.4% of global retail sales by the end of 2022, up from only 10% five years ago [1]. In the past few years the COVID-19 pandemic accelerated the already steady growth of the e-commerce market. In times of uncertainty, fears of the virus and stay-at-home policies have driven changes in consumer behaviour, bringing offline consumers to online stores. According to the 2020 ARTS release, U.S. e-commerce sales increased by $244.2 billion or 43% in 2020, the first year of the pandemic, rising from $571.2 billion in 2019 to $815.4 billion in 2020 [2].

The exponential growth in the e-commerce market due to the COVID-19 pandemic comes with supply chain challenges. Consumer expectations are rising and services such as same day delivery and free returns are becoming the norm [3]. The rising consumer demand is leading to an increase in need for logistic labour. However, due to the pandemic a grand reassessment of essential job sectors has lead to a shortage of available logistics workers [4]. Robotic automation could be a solution for these challenges. Robots can help companies by conducing laborious or time consuming tasks such as picking and sorting of items. The usage of robots for these pick-and-place processes are being implemented more and more in different highly automated warehouses [5].

An example of such a robot is the Smart Item Robotics (SIR) system as seen in Figure 1.1a, which is made by Vanderlande [6] in collaboration with Smart Robotics [7]. At the end of the robot arm it uses a bellows suction cup for picking and placing numerous objects. The suction cup has an interesting shape as seen in Figure 1.1b which allows the robot arm to grab objects of various shapes, materials and masses. The objects that are referred to are rigid bodies, such as cardboard boxes used for distribution, with surfaces which allow for perfect sealing of the suction cup lip. Due to the fact that suction cups are able to pick and place such a large set of different objects, they are commonly used. In order to predict its behaviour while operating, the bellows suction cup dynamics are being investigated. The properties of the suction cup, such as the stiffness, are dependent on the internal air pressure at which it is operating. Using the different properties of the suction cup which result from different internal pressure levels is beneficial for certain scenarios.

(a) (b)

Figure 1.1: The Smart Item Robotics (SIR) system; (a) a robotic picking station; (b) example of a bellows suction cup which is used to pick objects.

1.2 Research goal

Altering the internal pressure level at which the suction cup is operating, changes its physical properties such as the stiffness. Exploiting these different properties of the suction cup is beneficial for different scenarios. Increasing the inflow pressure level increases the stiffness of the suction cup which makes it very rigid. This allows for a firm grip onto an object but low compliance. If a collision were to occur, it may well cause the grip between the suction cup and the object to break meaning the object would be dropped. On the other hand, decreasing the operating pressure would make the suction cup less stiff which results in increased compliance. This elastic behaviour would be beneficial for interaction with the environment since collisions with other objects would not necessarily cause the object which is being held to be dropped. Higher compliance also means the system can better handle large uncertainties. This is for example useful when densely filling a tote box with many boxes of which their geometry and pose are known but with large uncertainties. It can be concluded that altering the internal pressure, directly influences the stiffness of the suction cup which is beneficial for different objectives.

Therefore the goal of this research project is to model the influence of the internal pressure on the stiffness of the bellows suction cup by means of data collection on the suction cup deformation. Experimental measurements are conducted to derive the suction cup deformation due to payload for varying internal pressure. A data collection procedure is constructed to store the experimental measurement results properly. Collected data is then analysed and evaluated in order to model the suction cup as the internal pressure changes. The goal of this research can be formulated as follows:

Develop, identify and validate a model which describes the 1D linear stiffness of a bellows suction cup at varying the internal pressure from collected experimental elongation measurement data.

1.3 Report structure

This report consists of six sections, of which the first is intended to introduce the project background and formulate the research goal. Section 2 regards literature research into the topic of modelling suction cup dynamics and similar research. In Section 3 the experimental setup and the experimental procedure are discussed in detail. Section 4 is devoted to formulate the modelling approach for modelling the suction cup for varying pressure. The results of the experiments with the applied modelling method are elaborated on in Section 5. In Section 6 the conclusions on the influence of the internal pressure on the stiffness of the suction cup are discussed. Finally, the recommendations which result from this research are posed.

2 Literature research

In this chapter literature research has been conducted into the usage of suction cups in robotics. Some studies which use different approaches for suction cup modelling are investigated. Furthermore, the I.AM. project which focuses on impact-aware manipulation in robotic logistics, is elaborated on.

2.1 Suction cup modelling

Suction cups are widely used in robotics because of their flexibility and applicability. Due to their unique shape and functionality, suction cups are able to hold objects consisting of various shapes, materials and masses. Even though suction cups are widely used in robotics, the literature is underdeveloped.

In [8], a novel interactive physically based approach for simulating active suction cup phenomena using a constraint-based formulation, was proposed. The suction cup is simulated using the finite element method (FEM) while the pressure is modelled with a constraint under the suction cup. This gives a clear understanding to the functionality of suction cups in robotics. In [9], further research was conducted for evaluating the simulation under various boundaries conditions or types of contacts with the environment. Here a novel physics-based model of the suction phenomenon between elastic bodies was presented. A constraint-based formulation was used to model pressure and contact between objects, while the deformation of the suction cup was achieved using the FEM. With this approach they were able to simulate suction phenomena for various scenarios, such as different types of suction cups and curved surfaces.

In [10], the leakage of suction cups was studied both experimentally and using a multiscale contact mechanics theory. The study shows that the suction cup volume and suction cup stiffness are important design parameters, but most important is the elastic modulus of the suction cup material, as a low modulus can drastically help in reducing gas (or liquid) leakage. In the end an improved bio-mimetic design of suction cups, inspired by octopus vulgaris, was suggested and is show in Figure 2.1. This improved design could show improved failure time underwater and on surfaces with varying degrees of surface roughness. It can be noticed that the shape of this improved design with wall springs highly represents the shape of a bellows suction cup as seen in Figure 1.1b. This design would allow for improved failure time on surfaces with varying degrees of surface roughness.

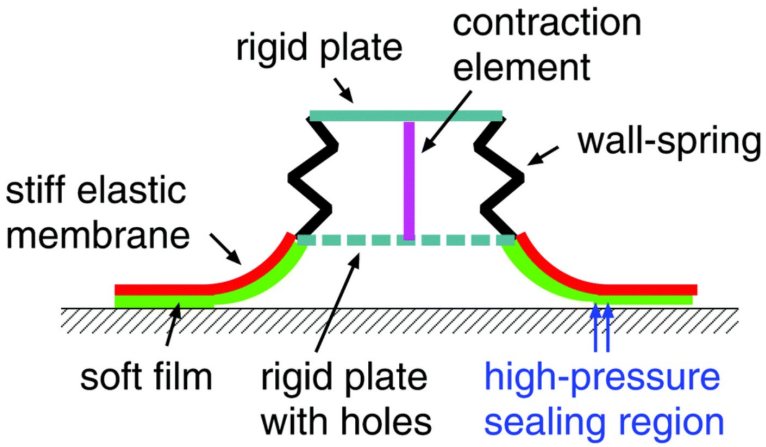

Figure 2.1: Octopus inspired suction cup from [10]

In [11], a prediction method for the inner air pressure of the suction cup was proposed. To achieve this the model was based on Bernoulli equation. They were able to predict the internal air pressure of the suction cup with small error due to the large number of data. Here the focus was on predicting the internal pressure as it would decrease due to air leakage over longer periods of time. However, no literature has been found into the influence of varying internal pressure on the stiffness of suction cups for different objectives.

2.2 I.AM. project

This research project is in context of the Impact-Aware Manipulation project [12]. The I.AM. project is a project which focuses on impact-aware manipulation in robotic logistics. The goal of the project is to decrease the pick and place time of robotic picking systems to increase the working speed and the workforce productivity. I.AM. is researching the exploitation of intentional impacts for robotic manipulation and interaction with environment. An example of this is the use of collisions to optimise volume occupancy of tote boxes. Here, contact between objects by pushing could be used for densely filling a tote box with many boxes.

A study as part of the I.AM. project performed by Peeters [13], constructed a model on the bellows suction cup dynamics in the situation of the tossing of objects. For this a similar setup was used. Tossing objects instead of placing them could be a way to increase the working speed of a robotic picker. At the end of this research a couple of interesting recommendations were made with respect to the modelling of the suction.

- To improve the results from the stiffness and damping identification, as performed in this report, static measurement data could be added to the identification data set. Furthermore, the identification data set can be extended with measurement data of dynamic measurements with different weights.
- The validation of the model could be expanded by evaluating some static measurements for which the tool-arm is kept in a fixed pose. When keeping the tool-arm in a fixed pose, there will be no damping of the bellows suction cup. So, by evaluating the pose of the package with respect to the tool-arm, the spring model can be validated separately from the damping model. This can be done for several static measurements where the package mass can be varied and the tool-arm is kept in different orientations.

It is stated that to extend further research into the tossing of objects with the use of a bellows suction cup, static measurement data could be added to the identification data set. This is to improve the results from the stiffness identification. Furthermore, the derived spring model could be validated separately by evaluating static measurements. Since, this research project is on static measurements to identify and validate the linear stiffness of the suction cup, this could be useful for further research into the tossing of objects with the bellows suction cup.

2.3 Summary

Literature research has been conducted into related work on suction cups in robotics. However, no similar research was found into varying internal pressure to influence the stiffness of the suction cup for different scenarios. Furthermore, the I.AM. project of which this project is in context, is elaborated on as well as recommendations from a study conducted by Peeters [13] on the tossing of objects.

3 Experimental setup and measurement procedure

This chapter is regarding the experimental phase of the project. The experimental setup that was used during the project as well as the different steps which were taken to obtain the final results will be elaborated on. First, in Section 3.1 the experimental setup which was used throughout the project is described. After this an overview of the measurement procedure will be given in Section 3.2.

3.1 Experimental setup

For the experiments that were performed in this project, a specific experimental setup was used. This setup is located at the Vanderlande Innovation Lab on the campus of the Eindhoven University of Technology and consists of multiple components. These components are a robotic manipulator which uses a suction gripper, a motion capture system and a pressurised air supply. This section will elaborate on these components and their details.

3.1.1 Robotic manipulator

The main part of the setup is the robotic manipulator, the UR10 robot made by Universal Robots [14] as seen in Figure 3.1a. It has six degrees of freedom due to the six rotating joints each of which have a range of -360° to 360°. The UR10 can hold a maximum payload of 10 kg, has a reach of 1300 mm and an accuracy of 0.1 mm. It is used for a variety of tasks but for this project the focus is on picking and placing objects by using a suction gripper as end effector.

The UR10 robot can be controlled in various ways with the use of a control panel, the so called teach pendant. With the teach pendant, programs can be loaded to run complex dynamic motions for the end effector of the UR10, for example the picking and placing of objects. However for this project the focus will not be on dynamic motions but on static measurements. So the teach pendant is used to assign specific angles to each of the rotary joint to move the end effector to the desired position, and to control (activate/deactivate) the valve of the vacuum system, through the I/O signals, and pressurise the suction gripper.

3.1.2 Suction gripper

Attached to the end of the UR10 is a Smart Robotics [7] tool arm on which a suction cup can be connected. This suction cup is a bellows suction cup of type piGRIp S1-7 from Piab [15] and has multiple components which can be seen in Figure 3.1b. It consists of a connection point to attach it to the tool arm without leakage of air, three bellows which can compress due to the created vacuum, and a suction lip with foam which causes a sealed grip between the suction cup and the object that is to be picked.

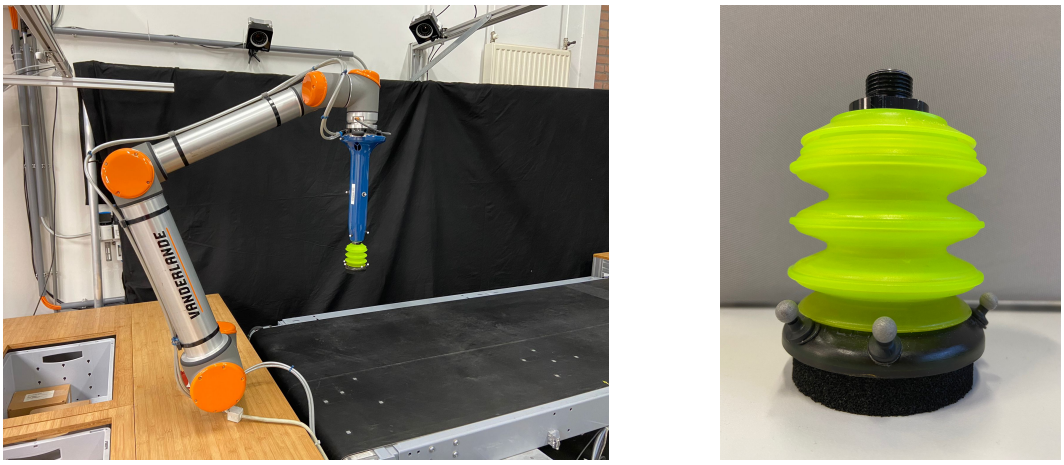

(a) (b)

Figure 3.1: Located at the experimental setup; (a) the UR10 Robotic manipulator; (b) the bellows suction cup.

The vacuum is created with the use of a pressurised air supply which is delivered by a compressed air tank near the setup. Inside the tool arm there is a blower that flows high pressurised air into a conical pipe with different section sizes as seen in Figure 3.2. In the figure the effect, which is called the Venturi effect [16], is shown for an air supply. The air flows from a region with a larger inner diameter to a region with a smaller diameter, causing the velocity to increase and the internal pressure to decrease below the atmospheric pressure ~ 1 [bar] in this region. Due to this reduced pressure, a vacuum is created which evacuates air from the end of the tool arm into the flowing air stream and blown out, as is on the left side of Figure 3.2. Without the suction cup attached to the tool arm, air will be sucked into the tool arm. However, when the suction cup is connected to the tool arm and the foam lip of the suction cup is pressed against the surface of an object, an airtight seal is created. This creates a force that allows objects to be picked. Increasing the inflow pressure decreases the internal pressure of the suction cup, meaning the pressure becomes more negative as it is a vacuum. Higher internal pressure means a tighter grip between an object and the suction cup.

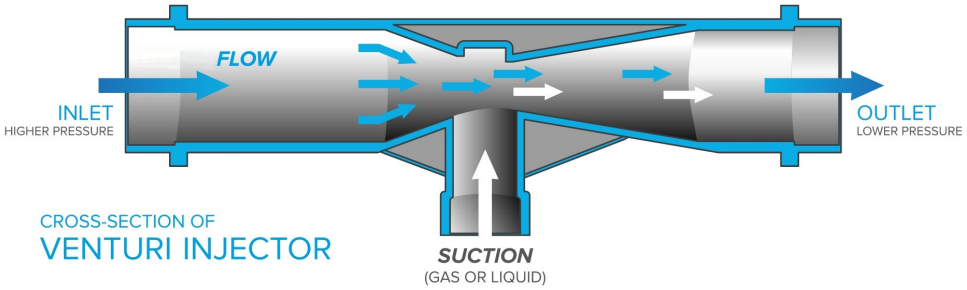

Figure 3.2: An illustration of a Venturi vacuum generator [16]

3.1.3 Motion capture system

In order to make measurements and get results from the experiments a motion capture system, or mocap system, is used. This system consists of six OptiTrack cameras [17], four Prime 17W and two Prime 22X cameras as seen in Figure 3.3a. These cameras are located around the experimental setup pointing towards the UR10. The cameras can track small markers by emitting infrared light which is reflected by the markers and captured again by the cameras. These markers are placed on specific positions of objects that are to be tracked. By placing markers in unique asymmetrical patterns, various bodies can be recognised and tracked by the system. By combing the information from all the cameras the position and orientation of multiple bodies, such as the tool arm and the suction cup, can be measured with an accuracy of 0.2 mm.

The software that is used to record the data is Motive [18]. Before recordings can be made the system has to be calibrated with the software using the CW500 Calibration tool from Figure 3.3b and the CS200 Calibration square as seen in Figure 3.3c. The calibration tool is used to calibrate the positions of the cameras with respect to each other. This is done by moving the tool in the visible space of the cameras while they are recording the motion. After this wanding procedure is done, the positions of the cameras have to be set with respect to a reference frame. This is done with the Calibration square which defines the reference frame in the virtual space of the setup. The Calibration square can be made level such that the vertical direction is well defined as the y-axis of the frame.

(a) (b) (c)

Figure 3.3: Components of the mocap system; (a) OptiTrack Prime 22X camera; (b) CW500 Calibration tool; (c) CS200 Calibration square.

3.1.4 Variable Inertia Object plate

In order to accurately perform measurements with a certain payload that was held by the suction cup, a variable inertia object plate, also named VIO plate, was used and is seen in Figure 3.4a. The VIO plate is made from plastic and has dimensions of 200x200x25 mm. It can be attached to the suction cup in order to confirm a tight grip between the suction cup and the plate and to assure the plate can not detach after it is loaded with high weight. Beneath the VIO plate, plates with holes in a 7 by 7 grid can be mounted as seen in Figure 3.4b. These grid plates can be loaded with weight by adding metal spheres with a diameter of 20 mm in the holes of the grid. This way the plates can act as baskets which can hold weight distributed over the surface of the plate. This can be used to perform experiments with off centred weight distribution and variable inertia. However, since this project is focused on 1D translation, the effect of variable inertia will not be investigated. Instead the construction of the VIO plate with a grid plate mounted beneath it is used as a basket to hold multiple spheres placed in a pattern to symmetrically distribute weight across the plate. The VIO plate together with one grid plate weighs 295g. Each sphere weighs 32.6g and a total of 49 spheres can be added in the holes of one grid plate. The VIO plate together with one loaded grid plate mounted onto the suction cup can be seen in Figure 3.4c.

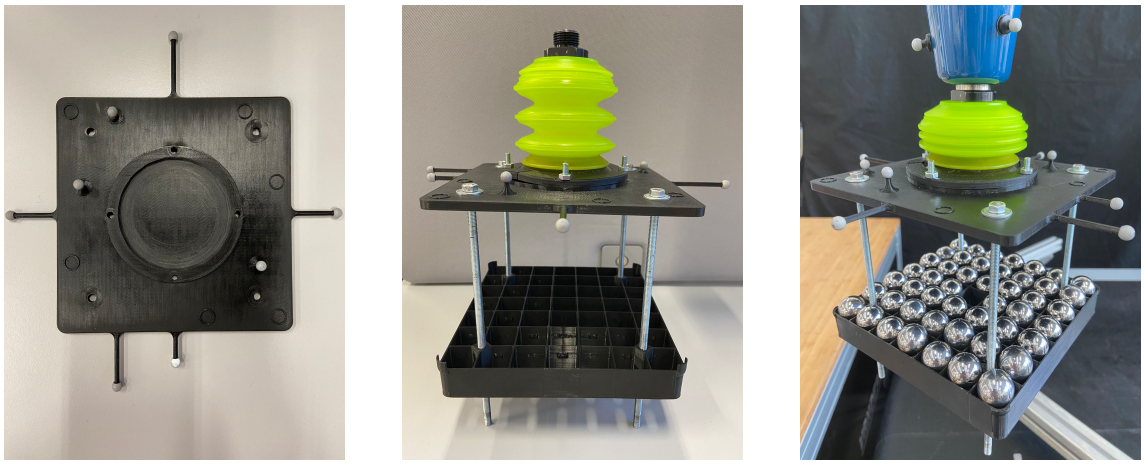

(a) (b) (c)

Figure 3.4: Measurement construction used for loading the suction cup; (a) the VIO plate; (b) the VIO plate with grid plate construction; (c) the VIO plate and loaded grid plate attached to tool arm.

3.1.5 Air flow regulator

The suction force at which the suction cup is operating can be adjusted. This is done by turning the valve of the regulator as seen in Figure 3.5a and changing the airflow to the tool arm of the UR10 robot. The regulator has a range from 0 to 10 bar. This is the pressure of the airflow into the system which creates the vacuum within the suction cup. The nominal operation pressure of the blower is 4 bars. Since the goal of this project is to investigate the influence of the internal pressure at which the suction cup is operating on the stiffness, the internal pressure is to be kept constant at each measurement. The pressure inside of the tool arm is measured by a VS-VP8-SA-M8-4 vacuum/pressure sensor made by

Schmalz [19]. It has a measuring range from -1 to 8 bar and gives an output in voltage from 0 to 10 volt. The output of the sensor is visible on the teach pendant as seen in Figure 3.5b. This value is different from the flow regulator and is given with a precision of two decimals. To keep the internal pressure constant the output value on the teach pendant should be watched and remain the same as well. There is no automatic regulator for the internal pressure so the sensor output value on the teach pendant has to be monitored visually to make sure the pressure levels stays constant. This is not an accurate way of keeping the internal pressure constant since adjustments are made after the pressure has already changed. This can be an issue and a potential source of error.

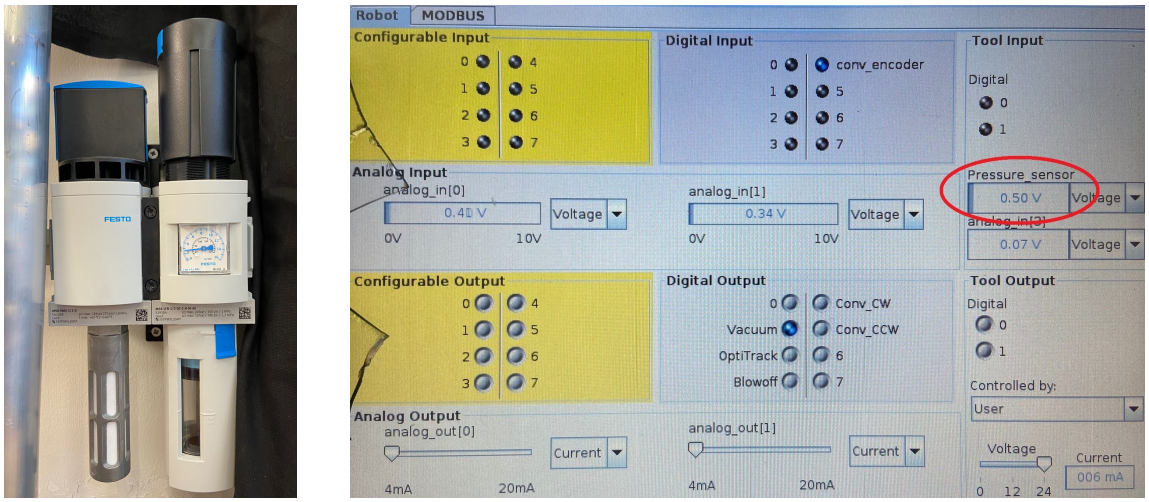

(a) (b)

Figure 3.5: For determining the operating pressure; (a) the regulator for adjusting the inflow pressure; (b) the teach pendant screen with internal pressure sensor output.

3.2 Measurement procedure and data storage

This section will elaborate on the measurements procedure that was followed to obtain the data and the data storage process. This procedure could be used when more experiments are to be executed for further research into suction cup modelling.

3.2.1 Measurement procedure

In order to execute the experiments a measurement plan was created and the following steps were followed:

1. The measurement procedure is started by running Motive and calibrating the OptiTrack cameras. By calibration the cameras, Motive computes the position and orientation of each of the cameras located around the setup. Also the camera lens distortions are determined as well as the mean error. The first step in calibrating the cameras is covering up all real reflective markers with pieces of paper or other available items. The remaining uncovered markers should be masked in Motive. Masking markers in the software filters out pixels from the data and has to be done with care. Filtering out excessive pixels may result in unwanted data loss.
   After covering the reflective markers, the wanding tool from Figure 3.3b should be used for the wanding process. By moving the wand around in the recording field of the cameras, samples are collected. Around 5000 samples per camera is sufficient for calculating the camera position and orientation. When the calculated result is "*exceptional*" it can be applied to the calibration. After the wanding process, the Calibration square from Figure 3.3c is used to set the reference frame. For this it has to be level and placed in the desired orientation. It uses a right-hand coordinate system with the longer end of the square pointing in the direction of the positive Z-axis, the shorter end towards the positive X-axis and the positive Y-axis pointing in the upward direction of the square. By selecting the calibration square markers and setting the ground plane, the calibration of the cameras is completed. The cameras have to be calibrated each time an experiment session is started. This is because the cameras could be moved as the setup is used often by many people, and to ensure to have accurate measurement results each time.

2. Once the calibration of the cameras is completed, the UR10 robot will be prepared for the measurements. The tool arm with the suction cup is attached to the robot and the VIO plate together with one basket plate is mounted onto the suction cup as seen in Figure 3.6a. The configuration of the robot is altered to put it in the desired position. For this, two important conditions have to be accounted for; First the suction cup with the VIO plate construction should be placed in sight of the cameras such that it is clearly visible. This is of importance as the position and the orientation of these components have to be measured. Moreover, the rotary joints of the robot should be positioned such that the direction of the centre axis of the tool arm is perpendicular to the XZ-plane that was set as a reference during the calibration phase. This way the axis of the tool arm is parallel to the Y-axis of the reference plane. This is important because of the fact that the measurements will focus on the 1D displacement in the direction of the Y-axis. As these two conditions are met, the robot has be prepared for the measurements.

3. Once the robot has been prepared for the measurements, the desired internal pressure that will be used for the experiment has to be set accordingly. As stated in Section 3.1.5 the internal pressure is to be kept constant during the measurements in order to get the desired results. The vacuum inside the tool arm is switched on and by reading the output value of the pressure sensor on the teach pendant and adjusting the flow regulator the internal pressure can be set to the desired value.

4. After the desired internal pressure has been set, the preparation has been completed and the experiment can be carried out. The experiment consist of loading the grid plate beneath the suction cup with weight while the vacuum is on and making recordings to measure the elongation in the Y-direction. The extra weight is added in multiple steps and after each step, a recording of a few seconds is made to measure the elongation for the current weight onto the grid. Starting with the unloaded construction of the VIO plate with one grid plate which weighs $\pm$295 gram, multiple spheres are loaded onto the grid in a symmetric pattern. Since there is a maximum of 49 spheres which can be added onto one grid plate, extra weighs are loaded on top of the spheres as can be seen in Figure 3.6b. This allows for a higher total weight which can be loaded onto the grid plate. The amount of weight which is loaded onto the grid plate per step varies per experiment as well as the total amount of weight that is loaded. This will be elaborated on in Section 5.1. An example can be seen in Figure 3.6c where six spheres with a combined mass of $\pm$196g were loaded per step onto the grid plate until a maximum of 48 spheres. To increase the total weight, six disks of $\pm$200g and one disk of $\pm$500g were added to allow for a total mass of $\pm$3569g. Once the total mass is reached, the weights are removed in the same steps until the grid plate is empty again. This process of loading and unloading the construction with weight is repeated a few times in order to get sufficient amount of data and to asses the presence of elastic hysteresis phenomena.

5. During the loading and unloading of the grid plate with weight, after each step a short recording is made to measure the position of the VIO plate as well as the position of the tool arm. This is done by running a program from a Linux PC located near the setup. This PC allows multiple components such as the UR10 and the mocap system to be controlled at the same time. This way each component does not need individual control by hand but instead can be controlled by running a program. For this project a program was made which would keep the vacuum turned on, make a mocap recording of 5 seconds and collect the data in folders when executed. This allows for efficient data collection during the experiments. The data collection will be elaborated on in the next section.

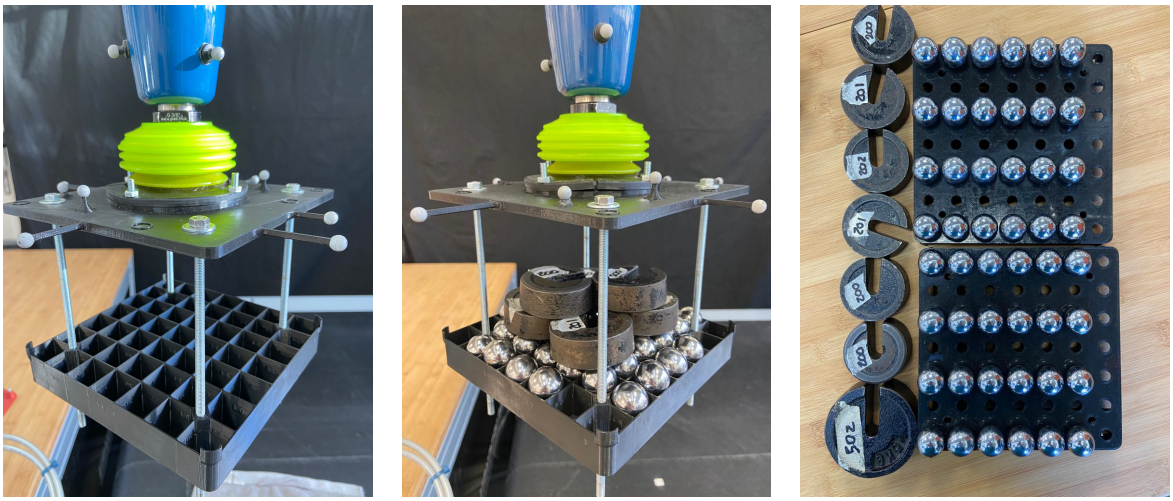

(a) (b) (c)

Figure 3.6: Measurement configuration; (a) the VIO plate with one unloaded grid plate attached to the suction cup; (b) the VIO plate with one grid plate loaded with weights; (c) weights used for the experiment

3.2.2 Data storage

During this project, multiple experiments were executed resulting in a large amount of data. In order to analyse the obtained data, it has to be stored properly. Each recording that was made during the experiments has two type of data sets, the motion capture data and the robot data. The mocap recordings are saved as .tak files by the Motive software and have to be converted to .csv files in order to analyse them with the use of Matlab. The robot data is also saved as a .csv file. By ordering the mocap data with the corresponding robot data of each recording in folders with the correct metadata about the experiments, an archive can be constructed. This archive stores all the data as a .hdf5 file together with the used setup description and sensor output such as the pressure sensor output. When the h5 archive is created, the script makes a transformation such that the z-axis points upwards. With the use of Matlab, the data in the h5 archives can be analysed.

3.3 Summary

In this chapter the experimental setup at the Vanderlande Innovation Lab that was used throughout the project has been discussed in detail. The robotic manipulator with the suction gripper as end effector and the air flow regulator have been presented and their functions explained. The motion capture system used to make recordings of the tracked objects such as the VIO plate, have been described. The measurement procedure that was used in order to do experiments is presented in steps. Finally the storage of the multiple data sources has been clarified.

4 Modelling method

In this chapter the method of the suction cup modelling will be presented. First the relation between the pressure sensor output and the internal pressure of the suction cup is described. Since the research goal is to investigate the influence of the internal pressure on the 1D deformation of the suction cup, the suction cup will be modelled as an elastic spring with the use of Hooke's law. Lastly, the method to derive the deformation of the suction cup from the measurements, is defined.

4.1 Vacuum/pressure sensor

As described in Section 3.1.5, the airflow into the system which creates the vacuum at which the suction cup is operating, can be adjusted. This is done with the use of the air flow regulator as seen in Figure 3.5a. Since the airflow into the system determines the internal pressure of the tool arm and suction cup, the relation between these different pressure levels is investigated. Measurements have been done where the airflow is adjusted to a certain pressure with the use of the regulator, after which the sensor output of the vacuum/pressure sensor belonging to this inflow pressure is noted. This has been done for multiple values of inflow pressure and the result can be seen in Figure 4.1a. It can be seen that there is a linear relation between the inflow pressure and the pressure sensor output which is described by

$$P_{volt} = -0.1060 \cdot P_{inflow} + 0.8672, \tag{4.1}$$

where the inflow pressure is given in bar and the sensor output in volt. The range of pressure which is to be investigated for this project is determined to be inflow pressure from 2.0 to 4.0 bar. This is because of two reasons. First the upper boundary of 4.0 bar is determined since this is the nominal pressure at which the blower in the suction gripper operates. Secondly, the suction force created by the vacuum is very small, so the suction cup is only able to carry light objects. From previous measurements it was found that with an inflow pressure below 2.0 bar the suction force is too low to perform experiments. So the lower boundary of the inflow pressure range was set to 2.0 bar. This results in a range of 0.44 to 0.67 volt of the pressure sensor to be set for the experiments. However, when investigating the vacuum/pressure sensor, a different relation can be found in the datasheet of the pressure sensor as seen in Figure 4.1b [19]. From this figure a linear relation of the form $y = ax + b$ was derived with the use of points (8,10) and (-1,0) to derive the parameters

$$a = \frac{\Delta y}{\Delta x} = \frac{10 - 0}{8 + 1} = 1.11, \qquad b = 0.9, \tag{4.2}$$

which are used to determine the relation

$$P_{volt} = 1.11 \cdot P_{internal} + 0.9 \qquad \Rightarrow \qquad P_{internal} = \frac{P_{volt} - 0.9}{1.11} \tag{4.3}$$

such that the internal pressure measured in voltage can be linked to a pressure value in bar. With the inflow pressure range of 0.44 to 0.65 volt, the internal pressure range of the suction cup at which experiments will be executed is determined to be from -0.414 to -0.235 bar with respect to the atmospheric pressure.

For the measurements on the internal pressure of the suction gripper, it is assumed that the inflow pressure remains constant.

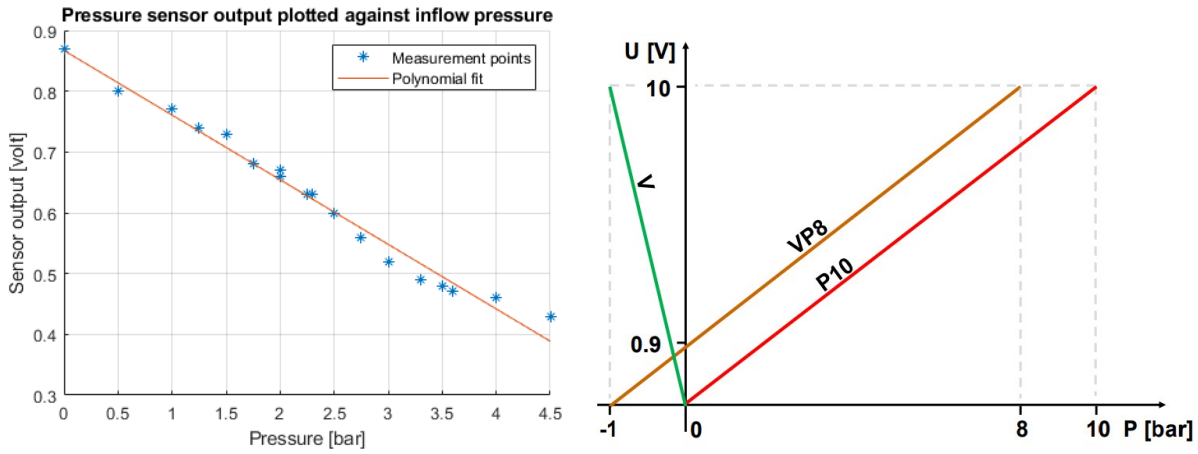

(a) (b)

Figure 4.1: For determining the pressure levels; (a) pressure sensor output plotted against inflow pressure from measurements; (b) vacuum/pressure sensor output in volt against internal pressure in bar as reported on the datasheet [19].

4.2 Hooke's law

The bellows suction cup which is used as the end effector of the robotic manipulator can be modelled as a spring. A spring is an elastic object that produces a restoring force when the spring is deformed by a deformation force caused by either compression or extension. The restoring force acts to restore the deformed spring in its equilibrium position [20]. The deformation can be an elastic deformation where the object will return to its original shape when the deforming force is removed, or a plastic deformation where the shape of the object will be permanently changed due to the force. In Figure 4.2 a typical stress-strain curve is shown for an arbitrary material. Stress σ is force per unit area and strain ϵ is the ratio which describes the deformation of an object with respect to its original form. When stress is applied to an object, the object will initially deform elastically as is shown for the dark grey area of the stress-strain curve until the elastic limit indicated by point B. This is the region, where the object will return to its original shape once the force is removed. When the force is increased beyond the elastic limit, the material will show plastic deformation where the object will have permanent deformation. For this project the focus will be on the region of elastic deformation since it is not meant to permanently deform the suction cup.

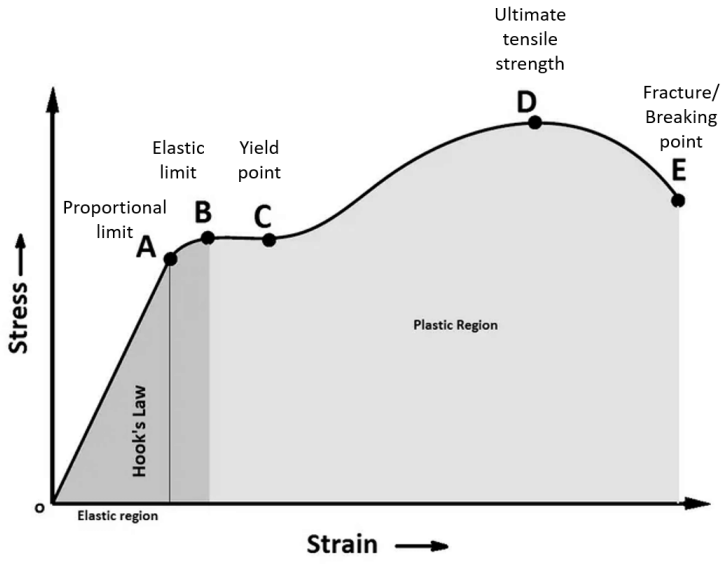

Figure 4.2: Illustration of a typical stress-strain curve.

Within certain limits the elastic deformation of the spring has a linear region for which the extension of the spring is proportional to the applied force. This is visualised in Figure 4.2 as the part from the origin of the curve until the proportional limit indicated by point A. This linear relation is known as Hooke's law and is written as

$$F_{spring} = -k \cdot x, \tag{4.4}$$

where F_{spring} is the restoring force exerted on the spring in Newtons [N], k is the spring constant in Newton per meter [N/m] and x is the extension or compression of the spring in meter [m]. The spring constant k is a measure for the stiffness of the spring. It is a material property and the larger the spring constant, the larger the resistance when extended or compressed. Since the suction cup is modelled as a spring, the spring constant, or the stiffness of the suction cup can be experimentally determined. Besides being a material constant, the stiffness of the suction cup is also dependent on the internal pressure caused by the vacuum. It can be observed that decreasing the internal pressure, so increasing the negative pressure caused by the vacuum, will increase the stiffness of the suction cup.

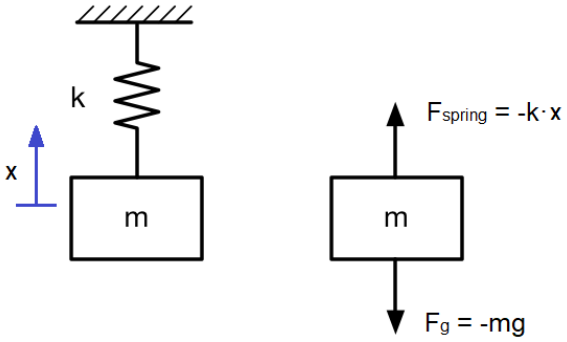

Figure 4.3: Free Body Diagram of the suction cup holding an arbitary object with mass.

For the bellows suction cup, the deformation force is the gravitational force which results from weight being loaded on the construction held by the suction cup. For the gravitational force it holds that $F_g = -m \cdot g$. Where m is the mass of the weight which is held by the suction cup and g is the gravitational acceleration. When an object with a certain weight is being held by the suction cup, the gravitational force and the spring force are in equilibrium as shown in the Free Body Diagram in Figure 4.3. From this equilibrium the expression

$$F_{spring} = -F_g \quad \Rightarrow \quad k = \frac{m \cdot g}{x}, \tag{4.5}$$

is derived for the stiffness of the suction cup, From the experiments, the extension x will be measured with the mocap system for the loaded mass. This way the stiffness of the suction cup can be experimentally identified for certain pressure levels.

4.3 Defining suction cup elongation

Due to the gravitational force acting on the payload being held by the suction cup, the suction cup is extended in the vertical direction. In order to determine the extension of the suction cup the relation

$$x = l - l_0, \tag{4.6}$$

is used where x is the elongation, l_0 is the nominal length and l is the total length of the expanded suction cup. The nominal length is defined as the length of the suction cup when the vacuum is turned on and a mass-less object would be held by the suction cup. Due to the created vacuum when the suction lip is sealed by an object, the suction cup will compress, as seen in Figure 4.4a. Increasing the mass of the object held by the suction cup, will increase the elongation in the vertical direction, as seen in Figure 4.4b. This relative extension is defined as a positive elongation since the length of the suction

cup from l_0 increases to l, which is equal to $l_0 + x$. So theoretically, by applying a mass-less object the nominal length of the suction cup can be determined. Since this is not possible, an object with a negligible mass of only 3g is used and the nominal length is defined.

With the nominal length of the suction cup defined, the elongation due to gravitational force can be determined. With the use of reflective markers located on the tool arm and the VIO plate, the position of these objects can be measured by the mocap cameras as discussed in Section 3.1.3. The tool arm is kept in place during experiments and assumed to remain still. This is to make sure the extension of the suction cup is not influence by motion and the 1D elongation can be measured accurately. During the experiment the load which is held by the suction cup will be increased causing the suction cup to extend in the vertical direction. This results in a lower position for the VIO plate with respect to the tool arm. The position is measured by the mocap system.

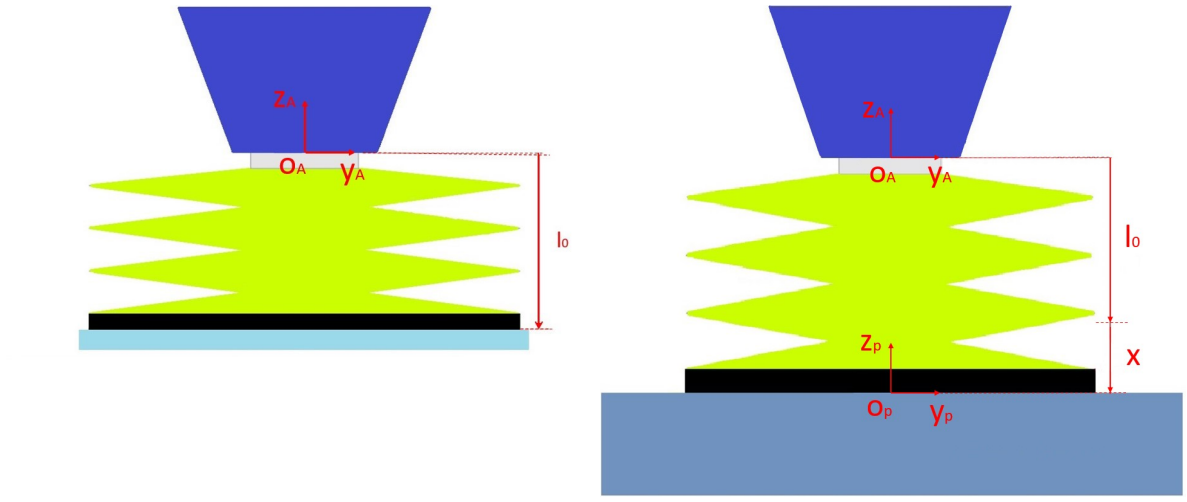

(a) (b)

Figure 4.4: Schematic representation of the suction cup; (a) illustration of the nominal length; (b) the suction cup with elongation due to applied load.

For analysing the measurement results certain frames are defined. Frame A is the coordinate frame fixed to the tip of the tooling arm where the suction cup is attached. Frame P is the coordinate frame fixed to the centre of the top of the VIO plate. During a recording the markers on the tool arm and the VIO plate allow the position and orientation of frame A and P to be measured. Each recording lasts for approximately 5 seconds which results in 1820 data points per recording for both frame A and P which are stored in the archive together with the data points from the other recordings from the experiment. With the use of Matlab these archives can be read and the average position of frame A and frame P are determined for each recording by taking the mean value. This is done because the tool arm is assumed to be motionless to focus on the elongation of the suction cup. So for each recording at a certain load and pressure level the average position of frames A and P are determined. By subtracting these values, the elongation is determined.

4.4 Summary

In this chapter the method which is used to model the suction cup is presented. A relation for deriving the internal pressure of the suction cup has been discussed. Moreover, the linear relation between the spring force and the extension described by Hooke's law is discussed as well as the relation to derive the stiffness of the suction cup at a certain load and pressure level. Lastly the method for determining the elongation of the suction cup from measurement results is outlined.

5 Results

In this chapter the results from the experiments will be discussed. Results from experiments to investigate the maximum load which could be held by the suction gripper, are presented. With the maximum load accounted for, experiments into the elongation of the suction cup in the vertical direction at a certain internal pressure level were executed. With the use of the modelling method determined in Section 4, the stiffness of the suction cup is modelled and the results are discussed. Noteworthy results are investigated and the final linear stiffness results per pressure level are elaborated on. With the linear stiffness results, the measurements are validated.

5.1 Maximum load

As discussed in Section 3.2, the amount of weight which will be loaded onto the basket plate per step varies per experiment as well as the total amount of weight that is loaded. In order to determine this, the total maximum load which could be loaded onto the plate is investigated. This was done altering the construction form Figure 3.4b by removing the parts that hold mounted the VIO plate to the suction cup. Removing these parts would allow for the loaded plate to detach from the gripper once the maximum load was exceeded. After removing theses parts more and more weight was added until the loaded plate becomes too heavy. At this point the gravitational force exerted by the weight becomes larger than the force created by the vacuum in the suction-cup. This procedure has been done for various internal pressures and the result can be seen in Table 5.1.

$P_{internal}$ [bar]	-0.396	-0.379	-0.368	-0.351	-0.341	-0.297	-0.270	-0.210
M_{max} [g]	> 3500	> 3500	3500	3200	2900	2700	2500	2050

Table 5.1: the maximum load for the linear elongation

With the maximum payload known for various internal pressure levels, the experiments into the elongation were executed by adding weight below the maximum. For these experiments the construction that keeps the VIO plate attached to the suction cup was mounted to the plate again, even though the maximum load would not be exceeded and the plate should not be supposed to detach from the suction cup. This is done as a safety measure and to make sure the connection between the VIO plate and the suction cup remains tight and the VIO plate remains attached when the vacuum is turned off in between experiments. With the known maximum load for each pressure the amount of weight that will be loaded in steps is also determined accordingly. For higher internal pressure, more weight is loaded per step and a larger total weight is loaded. This way the extension of the suction-cup can still be measured with sufficient amount of steps. For instance, at an internal pressure of -0.270 bar a total of 2085g was loaded in steps of 131g, and at an internal pressure of -0.396 bar a total of 3569g was added in steps of 200g.

5.2 First measurement results

Once the maximum load and the amount of weight to add each step has been determined, experiments were conducted as discussed in Section 3.2. During the experiments, mocap recordings of approximately 5 seconds are made by the cameras, which measure the position of both frame A and P at any corresponding load, as discussed in Section 4.3. The first experiment was executed with the inflow set to the nominal pressure of 4 bar. Starting from the unloaded VIO plate with a mass of 295g, 6 spheres with a combined mass of approximately 196g were added and a recording of five seconds was made. This was repeated until a total of 48 spheres were loaded after which disks with a mass of $\pm$200g and one disk with a mass of 502g were loaded to the plate. After this, the weights were removed in the same steps as they were added. This was repeated six times resulting in 166 recordings. The obtained data was stored in an archive which was analysed with Matlab by filtering the useful information. The mean position of both the VIO plate and the tool arm were determined per recording. The difference between these positions results in the elongation of the suction cup in the vertical direction due to the gravitational force acting on the loaded VIO plate. The elongation was plotted for each of the recordings and the result is seen in Figure 5.1.

From this figure a few things can be noticed. First of all, the five different loading and unloading phases can be recognised, where loading and unloading once forms a set of measurements, and each set

consists of 33 recordings. The five different sets are visualised in the figure by different colours and are indicated in the legend of the figure. The relative elongation of the suction cup is plotted on the left y-axis in mm, on the right y-axis the measured internal pressure is plotted in bar and on the x-axis the recordings that are made. It can be seen that the elongation is not defined correctly since the measurement results start with positive values, and decrease below zero. This is due to the fact this is a graph plotted with the raw values without post processing and properly accounting for the nominal length. The elongation is defined as the difference between total length and the nominal length of the suction cup as stated in Section 4.3. So Figure 5.1 shows the relative elongation, but without the right nominal length taken into account resulting in a vertical offset.

Furthermore, a large difference in relative elongation can be notice between the measurement sets. For the first set of loading and unloading the measured elongation ranges from -0.2 to -2.4 mm giving an elongation of the suction cup of 2.2 mm. For the second and third set the elongation ranges from -0.4 to -3.85 mm which results in an elongation of the suction cup of 3.45 mm, while for fourth and the fifth sets the elongation ranges from -0.1 to -1.4 mm resulting in an elongation of 1.3 mm. Since these measurements are done with the same weight it was not expected to find results which would differ almost a factor of three. This difference is caused by the difference in internal pressure. It can be seen that for set 1 the pressure remains constant around -0.389 bar for the first 23 recordings, with a spike in pressure level at the end of the set of recordings. For set 2 the internal pressure remains constant around -0.349 bar and set 3 around -0.346 bar.

Besides this difference in elongation, the linear elongation of the suction cup can be seen for the fourth and the fifth set of loading and unloading while the first three sets show mostly non-linear elongation.

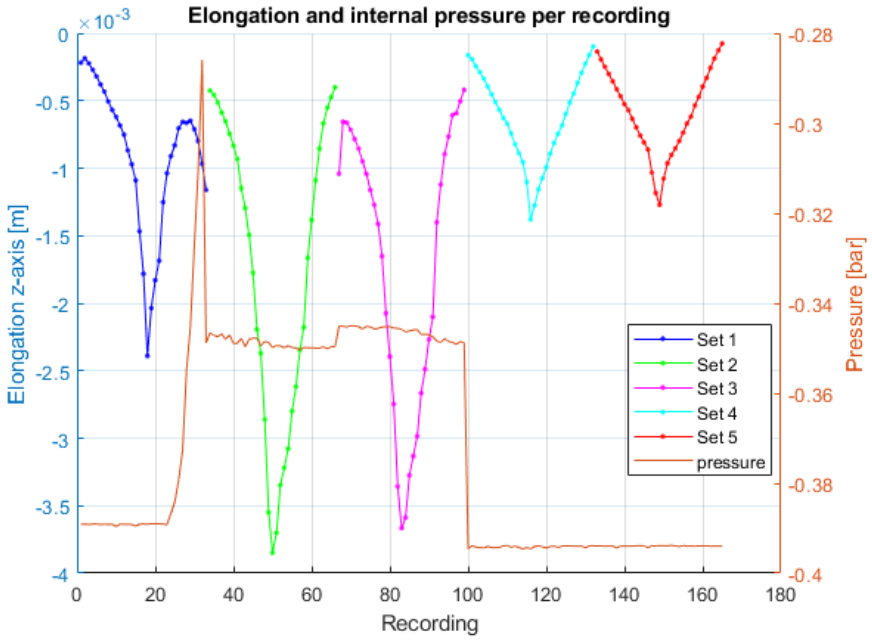

Figure 5.1: First experiment results at inflow pressure of 4 bar, elongation and internal pressure of the suction cup plotted at each of the 166 measurement points.

From the findings of the first experiment results, the elongation at an inflow pressure of 4 bar was further investigated. The fifth and sixth sets from Figure 5.1 are selected and the other sets are filtered out. This is done because of the fact that these two sets show comparable measurements for elongation at the same gravitational force while also resembling the linear characteristic. The elongation and the pressure sensor output per recording are plotted in Figure 5.2a. Here it can be seen that the pressure sensor output remains constant at an internal pressure of -0.394 bar and the elongation on the y-axis has been adjusted for the nominal length such that the elongation for a force of 0N would be 0 m. The elongation in vertical direction ranges from 0.1 to 1.4 mm with a slight deviation between the two sets. In Figure 5.2b the elongation in vertical direction is plotted against the gravitational force which results from different weights being loaded onto the VIO plate. It can be noticed that the y-axis is mirrored to

better show the increase in elongation due to the increase of gravitational force. For each specific weight, four recordings are made resulting in 4 data points at a specific weight, except for the maximum weight, for which only two recordings were made. The mean value of these results per weight is also plotted in the graph in black as well as a linear fit in cyan which is plotted for the force ranging from 2.894 to 28.125 N. The linear fit is not plotted for the whole force range because of the fact that for force larger than 28.125N, the behaviour of the suction cup becomes non-linear, as was also found by Peeters [13]. For force lower than 28.125N, a clear linear relation between gravitational force and vertical elongation can be seen. Since the goal of this project is to investigate the linear behaviour, this range was selected.

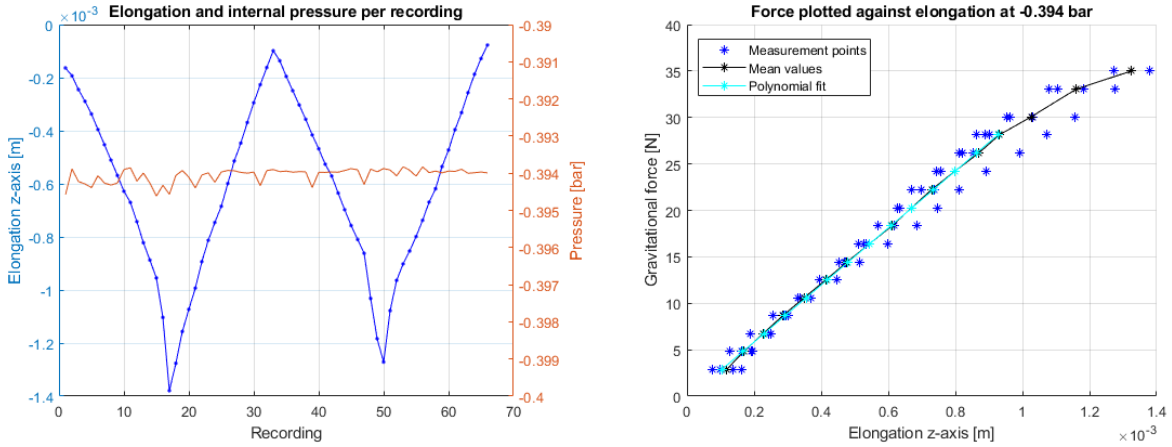

(a) (b)

Figure 5.2: At inflow pressure of 4 bar: (a) elongation and internal pressure sensor output plotted per recording; (b) elongation plotted against gravitational force.

With the use of (4.4) and the linear fit resulting from Figure 5.2b the stiffness of the suction cup at an inflow pressure of 4 bar and an internal pressure of -0.384 bar, could be determined to be equal to 30689 N/m. This result was compared with results obtained from earlier measurements into the suction cup with a slightly different setup. These measurements were executed by Dr. A. Oliva for research into the 6D modelling of the bellows suction cup. For these measurements a similar procedure was followed as described in Section 3.2 which resulted in measurements for the vertical elongation at a certain weight as seen in Figure 5.3. In this figure it can be seen that more recordings were performed at each of the selected weights at the same inflow pressure of 4 bar. The red dots show the elongation from loading weight and the blue dots for unloading. For a force ranging from 3.0215 to 27.959 N resulting in a vertical elongation from 0 to 1.4 mm From these measurements a mean value per weight was determined and plotted in black together with a linear fit plotted in cyan. With the use of (4.4) and the linear fit, the stiffness of the suction cup was determined to be 29828 N/m at in inflow pressure of 4 bar. When comparing the two results obtained from different experiments a difference of 861 N/m or 2.89% can be calculated. From this result it was determined that the number of measurement points used to obtain Figure 5.2b bar are sufficient to determine the stiffness of the suction cup at a certain internal pressure. With this knowledge, more experiments following the same measurement procedure were performed for certain pressure levels.

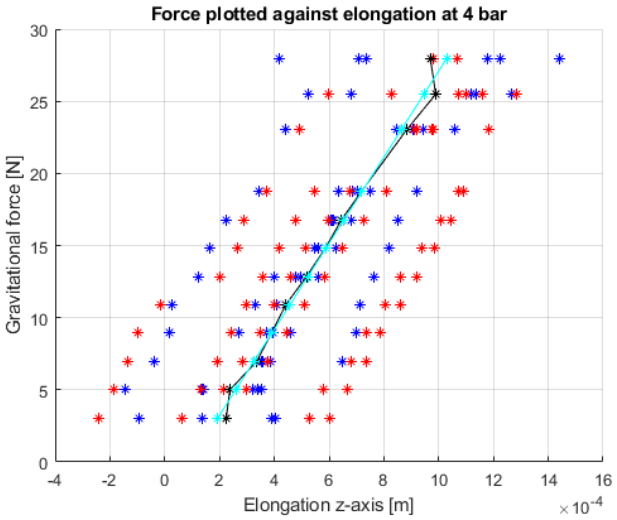

Figure 5.3: Measurement results obtained from similar research into suction cup modelling using a slightly different setup.

5.3 Further measurement results

From the first measurement results important conclusions were drawn regarding the data analysis. First it was concluded that the nominal length of the suction cup had to be accounted for properly to derive the elongation. Moreover, the method to derive the linear stiffness from the measurement results was determined and validated with the use of results from similar experiment. With the method validated, it was determined that the measurement procedure that was used to get the first results, was sufficient to determine the pressure at a certain pressure level. This procedure was repeated for experiments at 18 different pressure levels ranging from -0.397 to -0.210 bar. For each experiment at a given pressure level weight was loaded in a range of 20 to 35 steps until the maximum weight, ranging from approximately 1800g to 3500g, was reached. The weight was loaded and unloaded twice per experiment resulting in four recordings per weight (two for the maximum weight) and a around 40 to 70 recordings per experiment. The obtained data was stored in different archives and analysed with the use of Matlab. Plots were made with the elongation of the suction cup in vertical direction, together with the pressure sensor output per recording. Also the elongation is plotted against the gravitational force and a linear relation is derived. An example of this is shown in Figure 5.4 were the results of an internal pressure of -0.387 bar are presented.

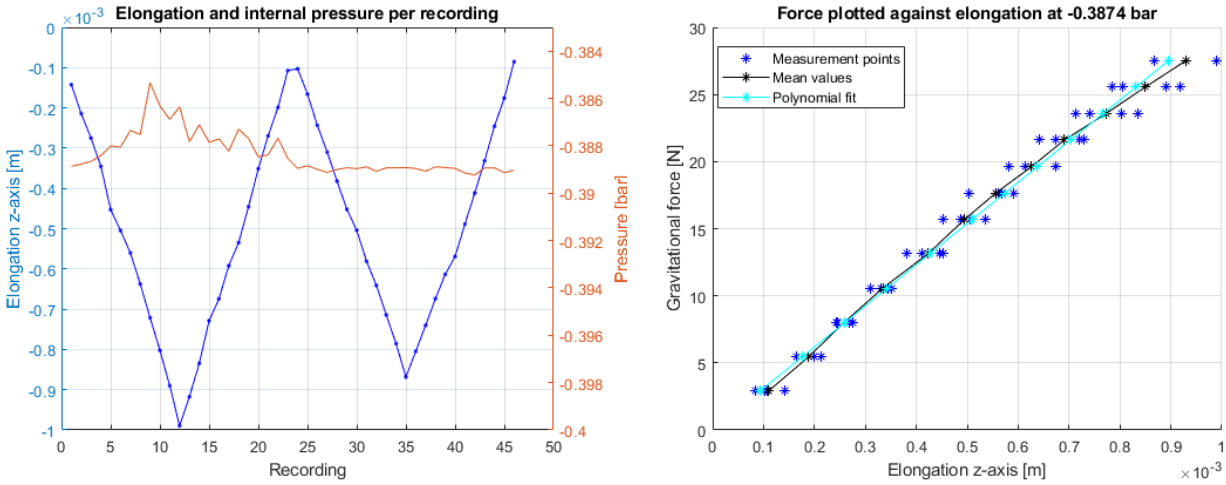

(a) (b)

Figure 5.4: Results at -0.387 bar: (a) elongation and internal pressure per recording; (b) elongation plotted against gravitational force.

For all the experiments at a certain pressure level these plots were made and can be seen in Appendix A.1. Some of the results that were obtained via this method showed different behaviour in comparison with other results. These different results will be discussed in the next section.

5.3.1 Non-linear behaviour

For each of the experiments, the linear relation between the elongation in the vertical axis and the gravitational force, as seen in Figure 5.4, was derived. When analysing the results it was found that for some experiments the VIO plate was loaded with weight beyond the linear characteristic. This is shown in Figure 5.5a were the elongation in vertical direction and the pressure sensor output are plotted per recording and in Figure 5.5b were the elongation is plotted against the gravitational force. For this experiment, the plate was loaded beyond the maximum load which could be held by the suction cup at an inflow pressure of 2.0 bar or an internal pressure of -0.21 bar. Due to this large payload the suction cup shows non-linear behaviour. When the gravitational force exceeds 10.5N, the slope of the curve changes and is no longer constant. Instead the results in the range of 2.66 to 10.5N are considered as this part of the curve is in the linear range of the suction cup. For this range a linear fit is plotted in cyan which could be used to determine the linear stiffness.

The non-linear characteristic due to high payloads, reoccurred for multiple experimental results. When this is noticed, the data is trimmed to the maximum load that obeyed in the linear range and a linear fit is plotted in this range. With the use of (4.4) the stiffness of the suction cup was calculated for each of the experimental results at a certain pressure level. These results are given in Table 5.2. Here the pressure sensor output in voltage, the internal pressure of the suction cup converted to bar and the calculated linear stiffness of the suction cup in N/m are presented.

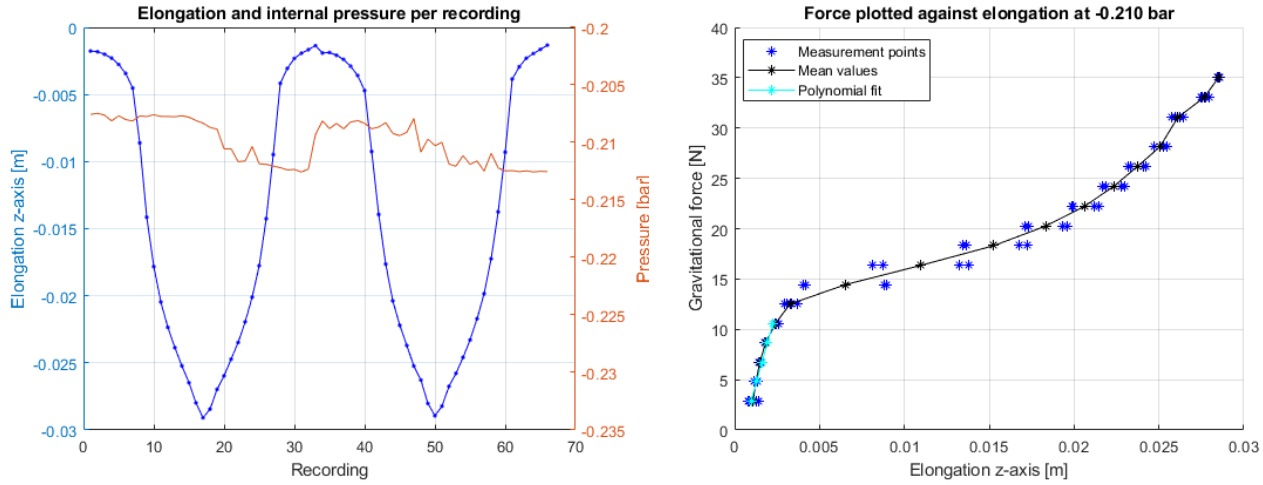

(a) (b)

Figure 5.5: Non-linear behaviour at -0.210 bar; (a) elongation and internal pressure per recording; (b) elongation plotted against gravitational force.

5.3.2 Measurements with changing pressure

As stated in Section 4.1, for the measurements on the internal pressure of the suction gripper, it was assumed that the inflow pressure would remain constant during the experiments. However, when analysing the pressure sensor output which was measured during the experiments, it was found that the pressure level changes over time. Even while the inflow pressure was put to a certain level by the pressure regulator from Figure 3.5a, the internal pressure measured by the sensor would sometimes change. For most of the experiments only little deviations in the pressure occurred which would not affect the results, as seen in Figure 5.5. However for a few experiments, larger deviations occurred as shown in Figure 5.6a. In this figure the elongation and the pressure sensor output per recording are plotted for an inflow pressure set to 2.7 bar. It can be seen that for the first few recordings the internal pressure increases after which it remains constant around -0.291 bar. At the sixteenth recording the pressure sensor output rapidly decreases to -0.305 and remains more or less constant around this level. While this change of -0.014 volt

is only a decrease of 4.6% it can be seen that it has a large influence on the elongation. For the first 15 recordings the elongation ranges from -1.37 to -2.42 mm, while after the change in pressure level it ranges from -0.585 to -1.77 mm. This results in an elongation of the suction cup of 1.05 mm for the first 15 recordings and an elongation of 1.185 mm for the remaining recordings which is a difference of 12.86%. In Figure 5.6b the elongation of the suction cup in vertical direction is plotted against the gravitational force. It can be seen that for each of the four recordings at a certain gravitational force, the measured elongation has a difference ranging from 1 to 2 mm. Because of the fact that there is such a large difference for recordings with the same force applied, which should result in a similar elongation of the suction cup, the results of this experiment are not reliable.

The experiment has been executed again were the pressure sensor output during the experiment was kept constant at a value of 0.57 volt for internal pressure of -0.297 bar. The measurement results are analysed and similar plots are made. In Figure A.13a it can be seen that the pressure sensor output per recording remains constant around 0.57 volt with small deviation. In Figure A.13b the elongation in the vertical direction is plotted against the gravitational force. For the measurements done at the same gravitational force, it can be seen that the deviation in elongation is reduced to values of 0.5 to 1 mm. This is an improvement compared with the results where the internal pressure changed over time as in Figure 5.6a and Figure 5.6b. These results were used to find the linear stiffness of the suction cup at this pressure level.

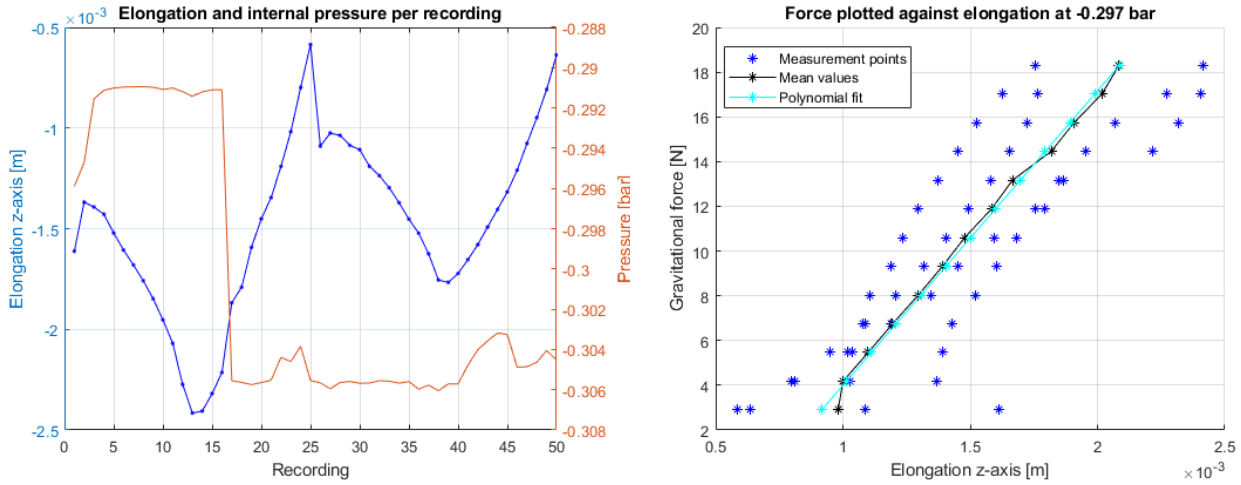

(a) (b)

Figure 5.6: Measurements affected by alternating pressure; (a) elongation and internal pressure per recording; (b) elongation plotted against gravitational force.

5.3.3 Influence of sunlight on mocap measurements

As described in Section 3.1.3 the motion capture system which is used to make recordings uses infrared light. The cameras emit infrared light which is reflected by the markers and captured again by the cameras. This way the position of multiple markers can be calculated and objects can be tracked. This is used to determine the elongation of the suction cup in the vertical direction due to the gravitational force. However, while doing measurements with the mocap system it could be noticed that the measurements could be influenced by excessive sunlight. At certain times during sunny days, sunlight would be reflected into the lab. This sunlight would reflect on some metal materials such as bolts located on the VIO plate or spheres used during the measurements. These reflections were observed by some cameras mistaking them for reflective markers. Because of the fact that these bolts used for constructing the VIO plate are close to some of the markers on the plate, the recordings would be affected with noise. Due to the reflected sunlight the measurements were influenced such that there were errors in determining the position of the VIO plate.

The influence of reflective sunlight on the measurement result is seen in Figure 5.7a where the elongation and the pressures sensor output are plotted per recording. In this figure it is hard to recognise a clear linear behaviour of the suction cup. Once the elongation is plotted against the gravitational force,

as in Figure 5.7b, the deviation between measurements at the same gravitational force becomes clear. A difference of almost 2mm in elongation can be seen for a force of 15N. Due to this large difference these experiment results are not reliable and no clear linear relation could be derived. The experiment at -0.324 bar was executed again without the influence of sunlight and similar plots were made. In Figure A.12a the vertical elongation and the pressure sensor output are plotted per recording and in Figure A.12b the vertical elongation is plotted against the gravitational force. For these results a smaller deviation of approximately 1mm in elongation at the same gravitational force can be seen. Furthermore a clear linear relation between elongation and force can be derived and is used to determine the stiffness of the suction cup for this pressure level.

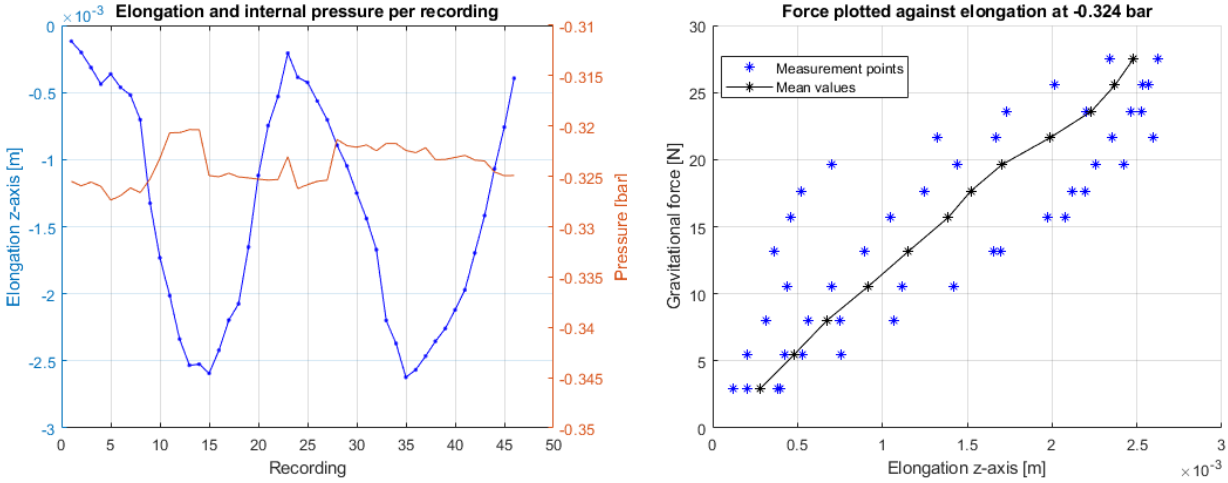

(a) (b)

Figure 5.7: Measurements affected by sunlight at -0.324 bar; (a) elongation and internal pressure per recording; (b) elongation plotted against gravitational force.

5.4 Linear stiffness results

As stated in the previous section, experiments were conducted for 18 different pressure levels. For each experiment the vertical elongation and the pressure sensor output per recording are plotted as well as the vertical elongation against the gravitational force as seen in Appendix A.1. All results are collected in Table 5.2, here the pressure of the airflow into the system is given in bar, the mean pressure sensor output for each experiment is given in volt, the internal pressure derived from (4.3) is given in bar and the calculated linear stiffness for each experiment is given in Newton per meter.

For each of the experiments at a certain pressure level, the linear stiffness is derived and plotted in Figure 5.8. In this figure a clear relation between the linear stiffness and the internal pressure of the suction cup can be observed. It can be seen that increasing the internal pressure of the suction cup, so reducing the vacuum which provides the suction force, results in a decreasing linear stiffness. In this figure a second-, third- and fourth-order polynomial are fitted for the data points. It can be noticed that the polynomial curves are close at each other for higher stiffness, but are deviating for lower stiffness. As the second- and fourth-order polynomial do not work well for lower stiffness, the third order polynomial is chosen to model the stiffness dependent on the internal pressure. The parameters of the third-order polynomial fit are as follows

$$\hat{k}(P) = -6.9566 \cdot 10^6 \cdot P^3 - 5.2135 \cdot 10^6 \cdot P^2 - 1.3169 \cdot 10^6 \cdot P - 1.0281 \cdot 10^5, \tag{5.1}$$

and can be used to model the linear stiffness of the suction cup at a certain internal pressure level.

P_{sensor} [V]	$P_{internal}$ [bar]	Stiffness [N/m]
0.46	-0.396	32346
0.4626	-0.394	30689
0.47	-0.387	29576
0.4739	-0.384	28323
0.48	-0.379	27280
0.49	-0.369	25213
0.4916	-0.368	23677
0.50	-0.360	20631
0.51	-0.351	17125
0.52	-0.342	15421
0.5217	-0.341	15055
0.54	-0.324	12788
0.57	-0.297	10558
0.5985	-0.272	10125
0.60	-0.270	10081
0.62	-0.252	9657.7
0.6287	-0.244	9222.1
0.667	-0.210	7873.4

Table 5.2: Per experiment: pressure sensor output, internal pressure of the suction cup and the derived linear stiffness from measurement results.

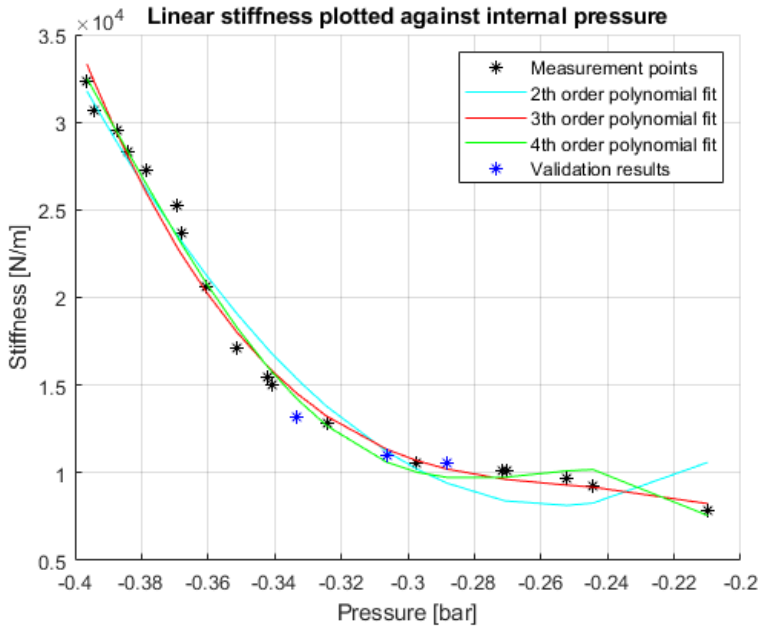

Figure 5.8: Linear stiffness plotted against internal pressure with validation results and a second-, third- and fourth-order polynomial fit.

5.5 Measurement validation

In order to research whether or not the measurement results and the model for the stiffness depending on internal pressure are credible, a validation procedure was conducted. This was done by investigating the vertical elongation at pressure levels for which no measurements were done before. At these pressure levels, the linear stiffness would be modelled with the use of (5.1). With the stiffness modelled, the vertical elongation at a given load could be estimated. Afterwards, for these pressure levels a similar procedure was followed as discussed in Section 3.2. Weight was loaded onto the VIO plate in steps and recordings were made for each of these steps in order to measure the actual elongation for the given load and pressure level. These results would be compared in order to validate the estimated stiffness.

For the validation procedure, internal pressure levels of -0.333, -0.306 and -0.288 bar were selected since no experiments were conducted at these levels yet. With the use of (5.1) the linear stiffness at the pressure levels has been estimated as $\hat{k}$, as seen in the second column of Table 5.3. For five different gravitational forces F_g from the the third column the elongation, $\hat{x}$, was determined with $\hat{k}$ and (4.4) as seen in the fourth column of the table. After this, experiments were conducted at the chosen pressure levels and the measurement results are show in Appendix A.2. In the fifth column of the table, the mean of the vertical elongation which was measured during the experiments at the same gravitational force, is given. These values have been corrected in order to account for the nominal length of the suction cup as stated in Section 4.3. The sixth column of the table presents the difference between the estimated elongation and the mean measured elongation in mm and the seventh column gives the difference as a percentage. It can be seen that the difference between the predicted elongation from the estimated linear stiffness and the mean measured elongation ranges from 0.03 to 16.2%. This error is in the order of 10^{-4} m which is the same order as the measurement accuracy of the mocap cameras, as stated in Section 3.1.3. Since the error for results at three different pressure levels and 15 different applied forces is this small, the measurement results and the model are deemed valid.

After the model is validated, the actual linear stiffness is derived for the results from the validation procedure and added to the table with the other measurement results as given in Appendix A.3. The results for the linear stiffness from the validation experiments are also plotted in Figure 5.8. It can be seen that the linear stiffness derived from the validation measurements is well in line with the other measurement results.

$P_{internal}$ [bar]	$\hat{k}$ [N/m]	F_g [N]	$\hat{x}$ [mm]	x_{mean} [mm]	$\lvert\hat{x} - x_{mean}\rvert$	error %
-0.333	14473	2.89	0.1997	0.206026	0.0063	3.18
		8.01	0.5535	0.559752	0.0063	1.14
		10.58	0.7310	0.759419	0.0284	3.88
		15.70	1.0848	1.14879	0.0640	5.90
		17.66	1.2202	1.31181	0.0916	7.51
-0.306	11311	2.89	0.2555	0.255439	0.0001	0.03
		8.01	0.7082	0.686908	0.0213	3.00
		13.14	1.1617	1.07709	0.0846	7.29
		17.66	1.5614	1.51348	0.0479	3.07
		21.61	1.9106	1.83227	0.0783	4.10
-0.288	10203	2.89	0.2832	0.196383	0.0267	9.49
		6.75	0.6616	0.449793	0.0968	14.6
		10.58	1.0369	0.758956	0.1677	16.2
		16.52	1.6191	1.23895	0.2296	14.2
		20.45	2.0043	1.58206	0.2671	13.3

Table 5.3: Results of the validation measurements compared to the estimated linear stiffness and elongation

With the linear stiffness determined for various internal pressure levels, the results are combined into Figure 5.9. On the axes of this figure the gravitational force, the vertical elongation and internal pressure are plotted. From all the results per pressure level the linear elongation is plotted due to the gravitational force at a specific internal pressure level. It can be observed that decreasing the internal pressure, so increasing the suction force created by the vacuum, increases the amount of force needed for the same elongation. In other words, decreasing the internal pressure increases the stiffness of the suction cup. This relation is in line with the results shown in Table 5.2 and it creates a surface in the 3 dimensional space.

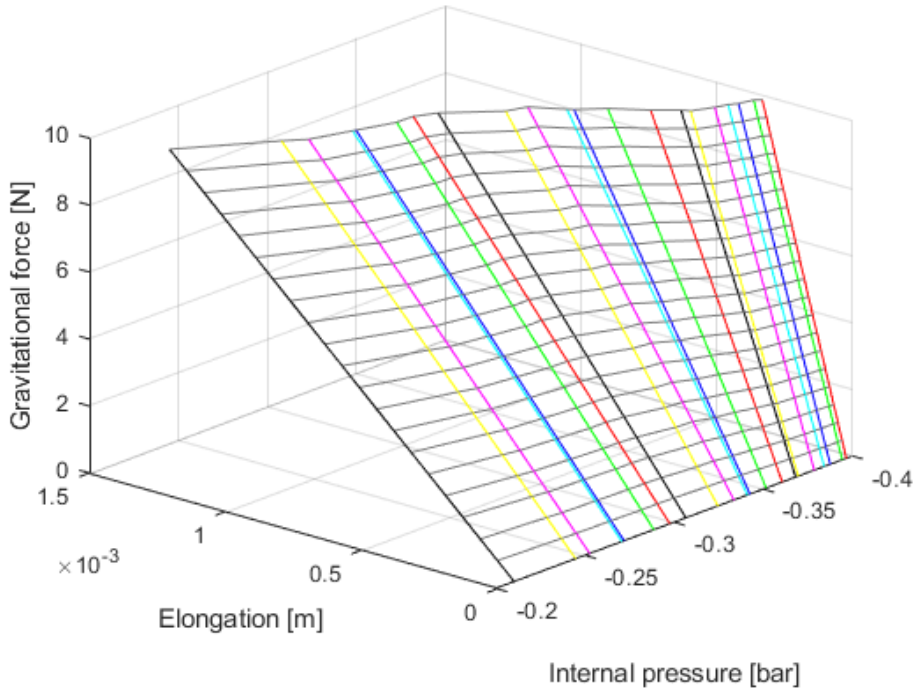

Figure 5.9: Force against elongation against pressure

5.6 Summary

In this chapter the results from the conducted experiments have been presented. The maximum load which could be applied per pressure level, is given. The first experimental results for the vertical elongation are investigated in detail to set the stage for more experiments. Experiments have been conducted for 18 different pressure levels and some interesting results are discussed. The linear stiffness is determined for every pressure level and the stiffness depending on the internal pressure is modelled. Lastly, the model is validated by a validation procedure and the total results are plotted in a 3 dimensional figure.

6 Conclusion and recommendations

In this chapter the findings from this project are revisited and a conclusion is drawn. Thereafter, recommendations are suggested for future research into the bellows suction cup.

6.1 Conclusion

In recent years, a steady increase in the worldwide e-commerce market has lead to an increase in demand for logistic labour. In the past few years, the COVID-19 pandemic has even accelerated this growth while leading to a shortage in logistic workers. Robotic automation in warehouses could be a solution to meet the increasing demand of supply chain. Laborious and time consuming tasks could be executed effectively by robots such as SIR system which uses a bellows suction cup for picking and placing objects. Exploiting the changing stiffness of the suction cup when varying the internal pressure levels is beneficial for different scenarios. Therefor the goal of this research project is to model the influence of the internal pressure on the stiffness of the suction cup by means of data collection of the suction cup deformation.

In this project, research has been done on the stiffness of a bellows suction cup for varying internal pressure. An experimental setup located at the Vanderlande Innovation Lab on the TU/e campus was used to conduct experiments. The setup consists of an UR10 robot with a suction gripper as end effector, surrounded by a motion capture system which was used to track the position of the robotic tool arm and the VIO plate. Experiments were done at different internal pressure levels and consisted of loading the construction beneath the VIO plate with weight such that the suction cup would have vertical elongation. Short recordings were made to measure the positions of the frames fixed to the tool arm and the VIO plate and stored into archives. The airflow supply creating the vacuum and the pressure sensor are investigated and a relation is derived to determine the internal pressure level of the suction cup. The method for modelling the stiffness of the suction cup with the use of Hooke's law is derived and applied on the measurement results. The maximum load per pressure level is determined and results for 18 different pressure levels are presented. All measurement results and some interesting findings are discussed. It was observed that the pressure level would sometimes change during experiments while the pressure was assumed to remain constant. Also the effect on sunlight on the OptiTrack cameras and the non-linear characteristic of the suction cup at high payload are discussed. For 18 different pressure levels the linear stiffness is determined and a relation for the stiffness dependent on the internal pressure of the suction cup is modelled. The model is validated for three new pressure levels at which no measurements were executed before. All the measurement results are collected in a 3D plot visualising the relation between vertical elongation due to gravitational force per pressure level. It can be concluded that increasing the inflow pressure, decreases the internal pressure of the suction cup as the pressure of the vacuum becomes more negative, which increases the amount of force needed for the same elongation. In other words, decreasing the internal pressure increases the stiffness of the suction cup.

In conclusion, a model which describes the 1D linear stiffness of a bellows suction cup at varying the internal pressure from the collected experimental elongation measurement data has been developed, identified and validated.

6.2 Recommendations

For further research into the modelling of the suction cup, some recommendations are made to overcome the problems encountered during this project .

First of all it is recommended to further investigate the system which is used for the pressure supply. For deriving the linear stiffness of the suction cup per pressure level, it was assumed that the internal pressure would remain constant. However, it was observed that this was not the case and the internal pressure would change during the experiment. For most experiments this would only be a minor change but for some experiments the deviation in pressure was actually large enough to influence the measurement results. Furthermore, in order to compensate for the changing pressure during experiments, the pressure sensor output has to be monitored. This way small deviations can be adjusted for with the use of the pressure regulator. However, the pressure sensor output is given on the screen of the teach panel where it is shown in voltage with only two decimals. Since experiments were conducted at pressure levels which are 0.01V apart, keeping the pressure at a constant level this way was quite hard. For further research it would be recommended to use a pressure regulator to ensure that the internal pressure of the suction

cup remains constant.

Moreover, it is recommended to improve the setup at the Vanderlande Innovation Lab with a mechanism to block sunlight. While doing experiments with the mocap system it could be noticed that the measurements could be influenced by excessive sunlight. At certain times during sunny days, sunlight could reflect on bolts of the VIO plate which could be mistaken by the cameras for reflective markers. This could affect the results with noise which could lead to possible measurement errors. In order to assure accurate measurement results during sunny days, it would be recommended to install blinds or a curtain to block sunlight coming into the lab.

The next step into modelling the suction cup dynamics would be to investigate the damping of the suction cup by performing dynamic experiments at varying internal pressure.

References

[1] P. Hung, "E-Commerce Trends 2022: What The Future Holds," Forbes Councils Member, March 2022. Available: https://www.forbes.com/sites/forbestechcouncil/2022/03/14/e-commerce-trends-2022-what-the-future-holds/?sh=7782a8858daf, accessed on 11-01-2023.

[2] M. Brewster, "Annual Retail Trade Survey Shows Impact of Online Shopping on Retail Sales During COVID-19 Pandemic," Census Bureau's Economic Management Division, April 2022. Available: https://www.census.gov/library/stories/2022/04/ecommerce-sales-surged-during-pandemic.html, accessed on 11-01-2023.

[3] Berkshire Grey Press, "Research Finds a Leading Cause of the Labor Shortage in Warehouses," BEDFORD, Mass, August 2022. Available: https://www.berkshiregrey.com/resources/press-release/berkshire-grey-research-finds-a-leading-cause-of-the-labor-shortage-in-warehouses/, accessed on 11-01-2023.

[4] R. Wilson, "How Ecommerce Answers the Ongoing Labor Shortage," Miva, June 2022. Available: https://blog.miva.com/ecommerce-answers-the-ongoing-labor-shortage, accessed on 11-01-2023.

[5] D. Edwards, "How Robots Can Contribute to the Ecommerce Industry," Januari 2022. Available: https://roboticsandautomationnews.com/2022/01/25/how-robots-can-contribute-to-the-ecommerce-industry/48610/, accessed on 11-01-2023.

[6] Vanderlande Smart Item Robotics (SIR), Available: https://www.vanderlande.com/systems/picking/smart-item-robotics/, accessed on 11-01-2023.

[7] Smart Robotics, Smart Item Picker. Available: https://smart-robotics.io/en/item-picking/, accessed on 11-01-2023.

[8] A. Bernardin, C. Duriez, M. Marchal. "An Interactive Physically-based Model for Active Suction Phenomenon Simulation." SWS19 - SOFA Week Symposium, Nov 2019, Paris, France.

[9] A. Bernardin, E. Coevet, "Constraint-based Simulation of Passive Suction Cups," Univ. Rennes, INSA, IRISA, Inria, September 2022.

[10] A. Tiwari, B. N. J. Persson, "Physics of suction cups," FZ Jülich, Germany, October 2019.

[11] Y. Tian, S. Ma, G. Kotani, "Inner pressure prediction of suction cup based on Bernoulli equation," Ritsumeikan University, September 2021.

[12] H2020 EU project I.AM. Available: https://i-am-project.eu/, accessed on 11-01-2023.

[13] G.J.H. Peeters, "On Modeling and Identification of Bellows Suction Cup Dynamics for Robotic Tossing," Eindhoven University of Technology Faculty of Mechanical Engineering, Dynamics Control Section, September 2021.

[14] UR10 robotic manipulator specifications. Available: https://www.universal-robots.com/media/50880/ur10_bz.pdf, accessed on 11-01-2023.

[15] Piab Bellows Suction-cup. Available: https://www.piab.com/en-us/suction-cups-and-soft-grippers/modular-suction-cups/pigrip-configurable-suction-cups/pigrip_g/#description on accessed on 11-01-2023.

[16] H. van Ormer, "Utilizing Venturi Vacuum Generators Efficiently," Air Power USA. Available: https://www.blowervacuumbestpractices.com/system-assessments/vacuum-generation/utilizing-venturi-vacuum-generators-efficiently, accessed on 11-01-2023.

[17] Optitrack Motion Capture Cameras. Available: https://optitrack.com/cameras/, accessed on 11-01-2023.

[18] Optitrack Motive, Optical motion capture software. Available: https://optitrack.com/software/motive/, accessed on 11-01-2023.

[19] Schmalz, Vacuum Technology from Schmalz. Available: https://www.schmalz.com/en/, accessed on 11-01-2023.

[20] Khan Academy, "What is Hooke's Law?". Available: https://www.khanacademy.org/science/physics/work-and-energy/hookes-law/a/what-is-hookes-law, accessed on 11-01-2023.

[21] M. Giuliodori, H. Lujan, W. Briggs, G. Palani, S. DiCarlo, "Hooke's law: applications of a recurring principle," December 2009. Available: https://journals.physiology.org/doi/full/10.1152/advan.00045.2009, accessed on 11-01-2023.

A Appendices

A.1 Measurement results

In this section the measurement results for all the conducted experiments are presented in similar plots. Experiments were done for a total of 18 different pressure levels for which a figure with the measured elongation and internal pressure are plotted per recording, plus a figure with the measured elongation plotted against gravitational force.

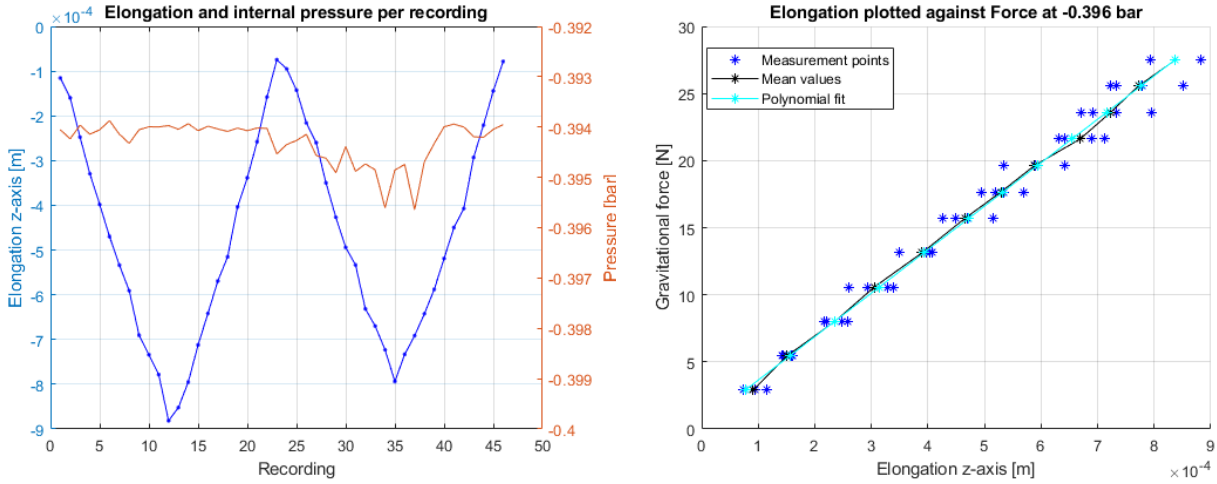

(a) (b)

Figure A.1: At -0.396 bar; (a) elongation and internal pressure plotted per recording; (b) elongation plotted against gravitational force.

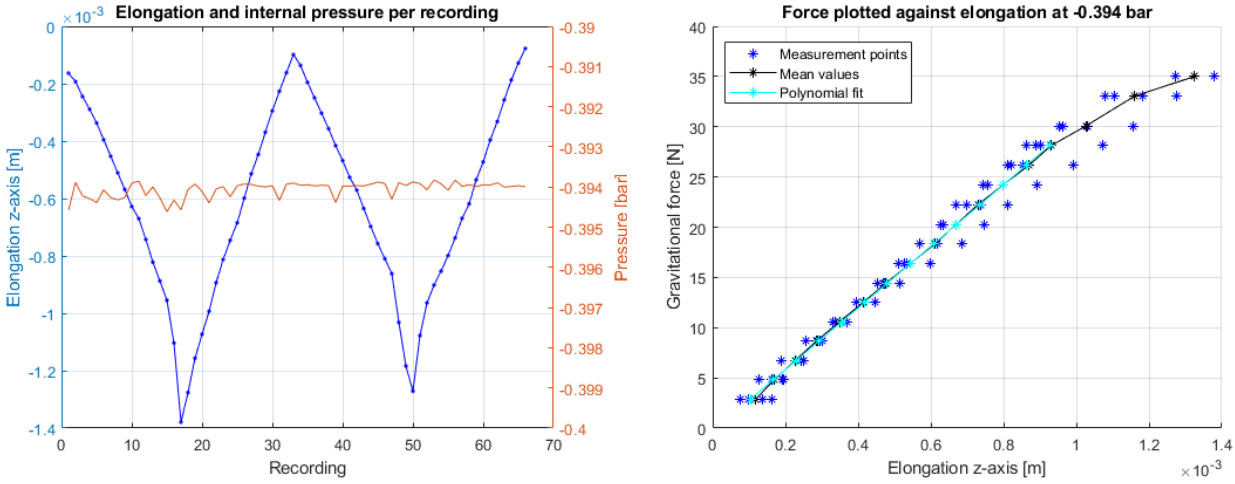

(a) (b)

Figure A.2: At -0.394 bar; (a) elongation and internal pressure plotted per recording; (b) elongation plotted against gravitational force.

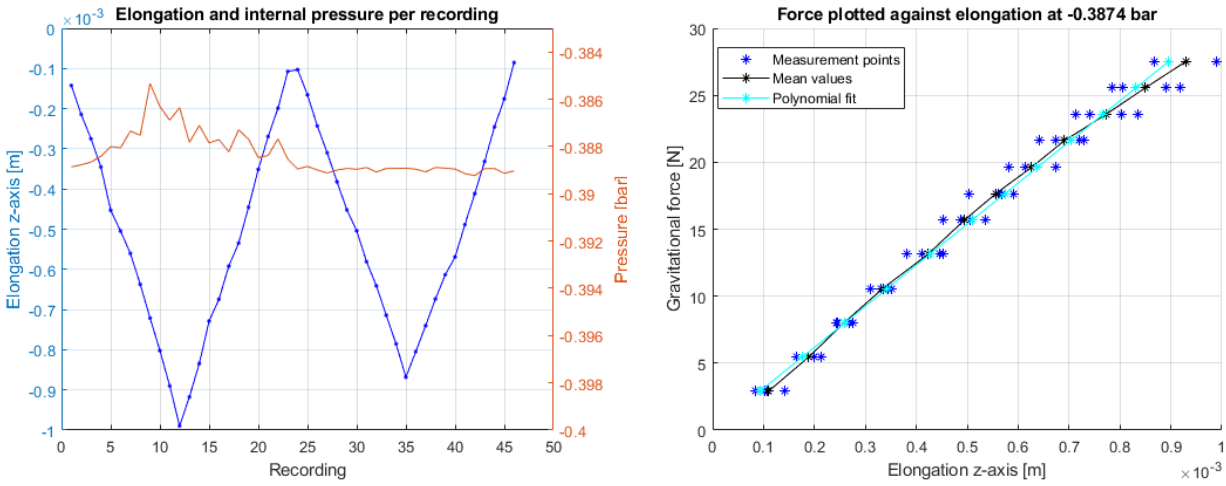

(a) (b)

Figure A.3: At -0.387 bar; (a) elongation and internal pressure plotted per recording; (b) elongation plotted against gravitational force.

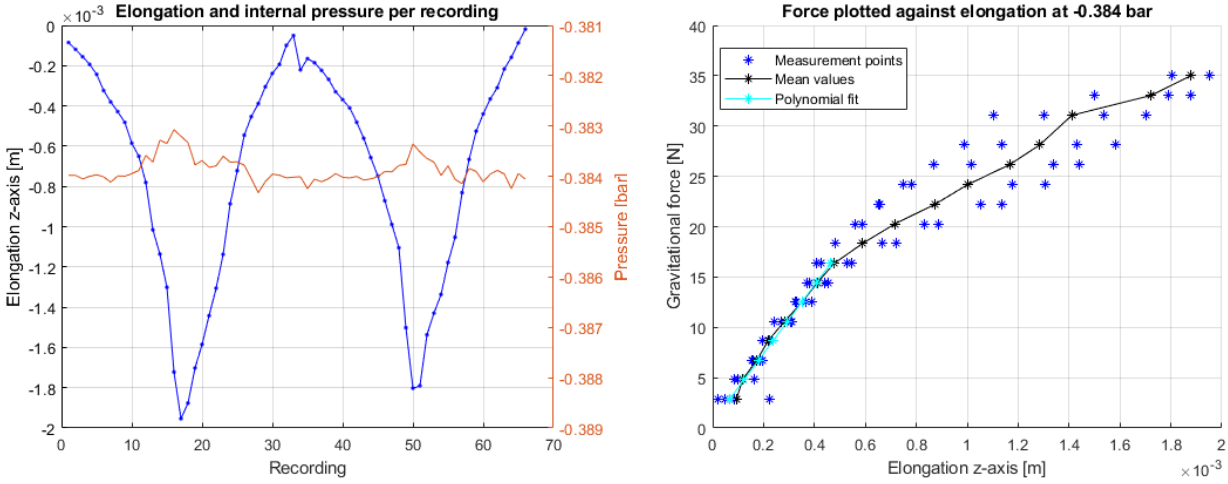

(a) (b)

Figure A.4: At -0.384 bar; (a) elongation and internal pressure plotted per recording; (b) elongation plotted against gravitational force.

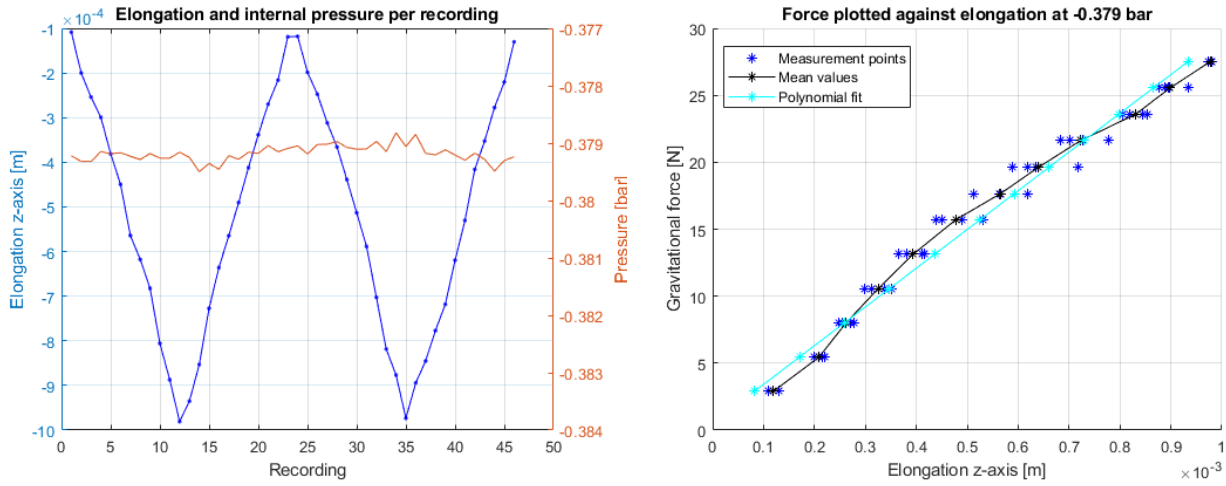

(a) (b)

Figure A.5: At -0.378 bar; (a) elongation and internal pressure plotted per recording; (b) elongation plotted against gravitational force.

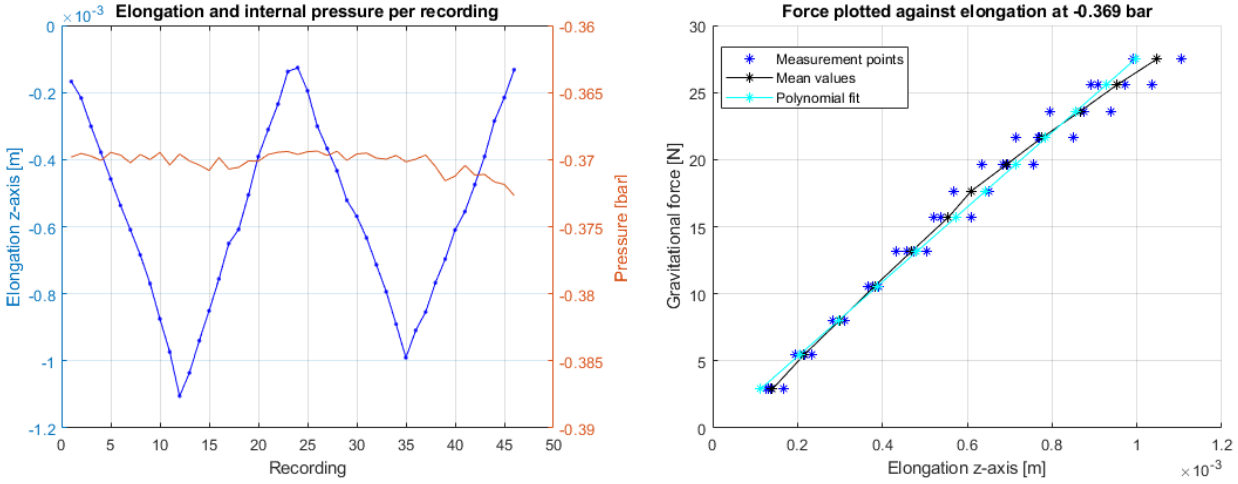

(a) (b)

Figure A.6: At -0.369 bar; (a) elongation and internal pressure plotted per recording; (b) elongation plotted against gravitational force.

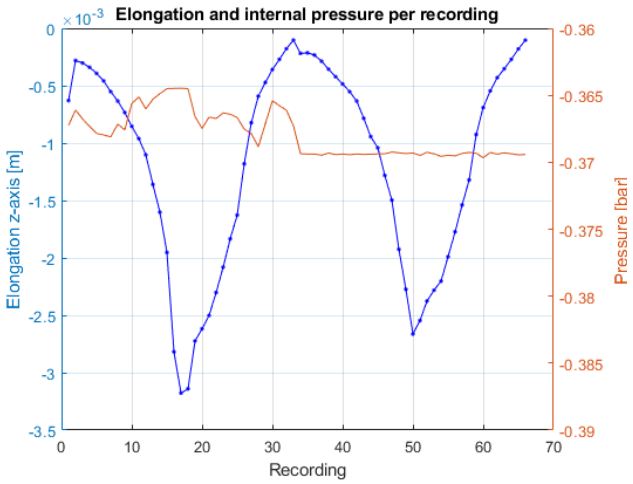

(a)

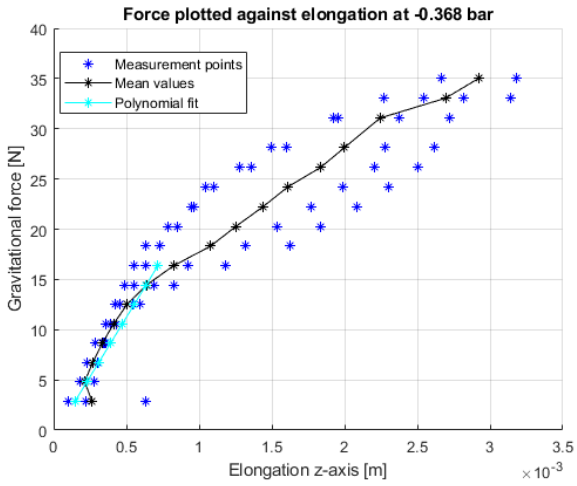

(b)

Figure A.7: At -0.368 bar; (a) elongation and internal pressure plotted per recording; (b) elongation plotted against gravitational force.

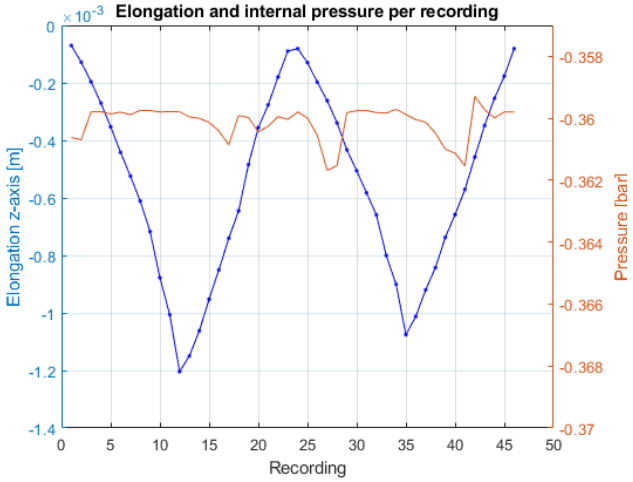

(a)

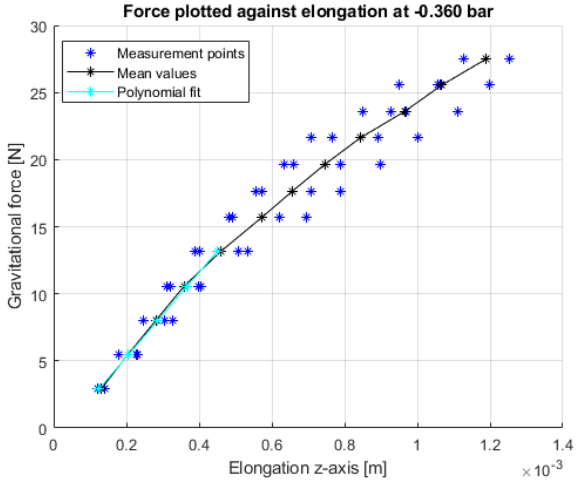

(b)

Figure A.8: At -0.360 bar; (a) elongation and internal pressure plotted per recording; (b) elongation plotted against gravitational force.

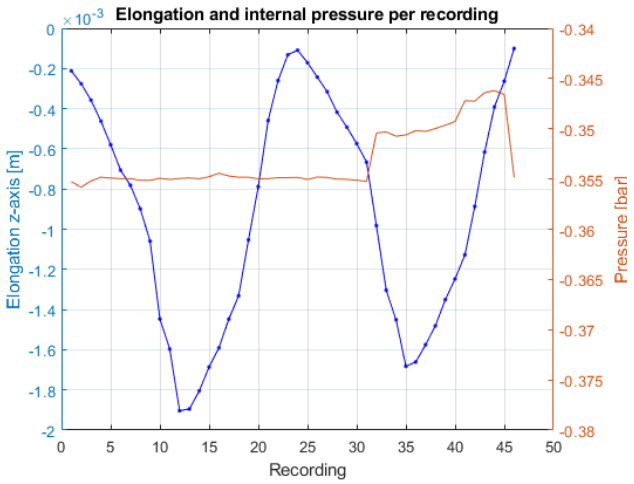

(a)

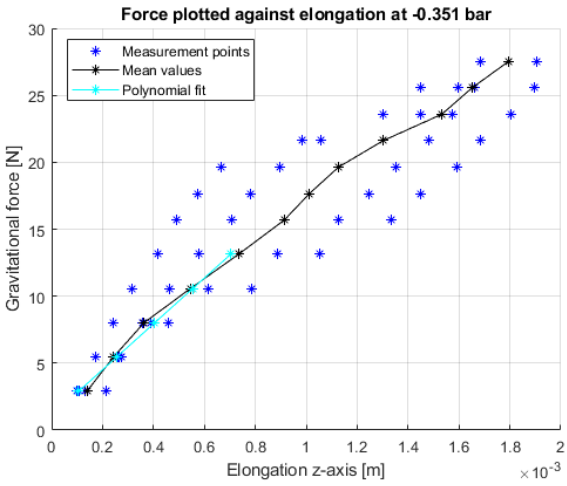

(b)

Figure A.9: At -0.351 bar; (a) elongation and internal pressure plotted per recording; (b) elongation plotted against gravitational force.

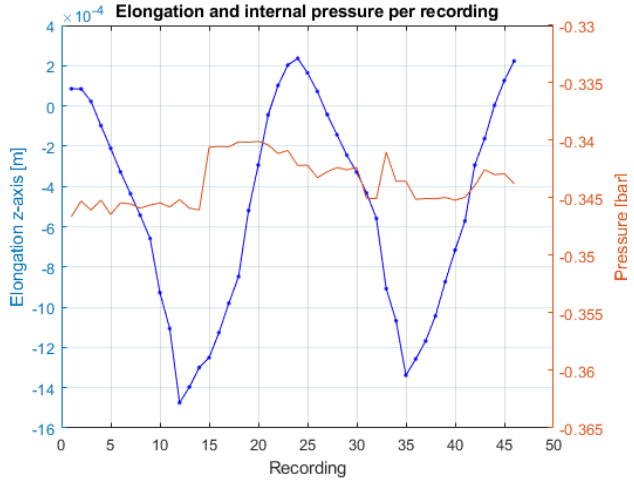

(a)

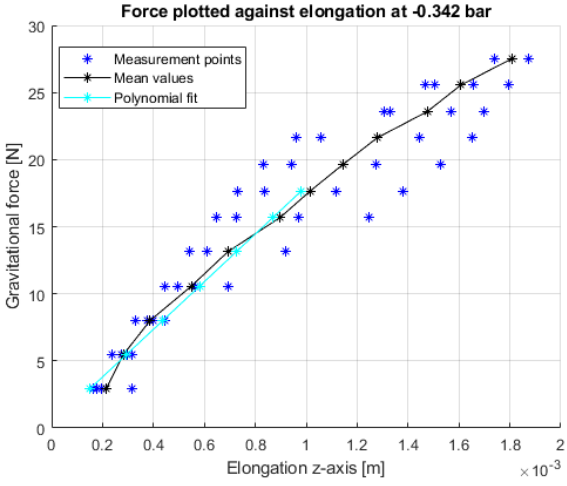

(b)

Figure A.10: At -0.342 bar; (a) elongation and internal pressure plotted per recording; (b) elongation plotted against gravitational force.

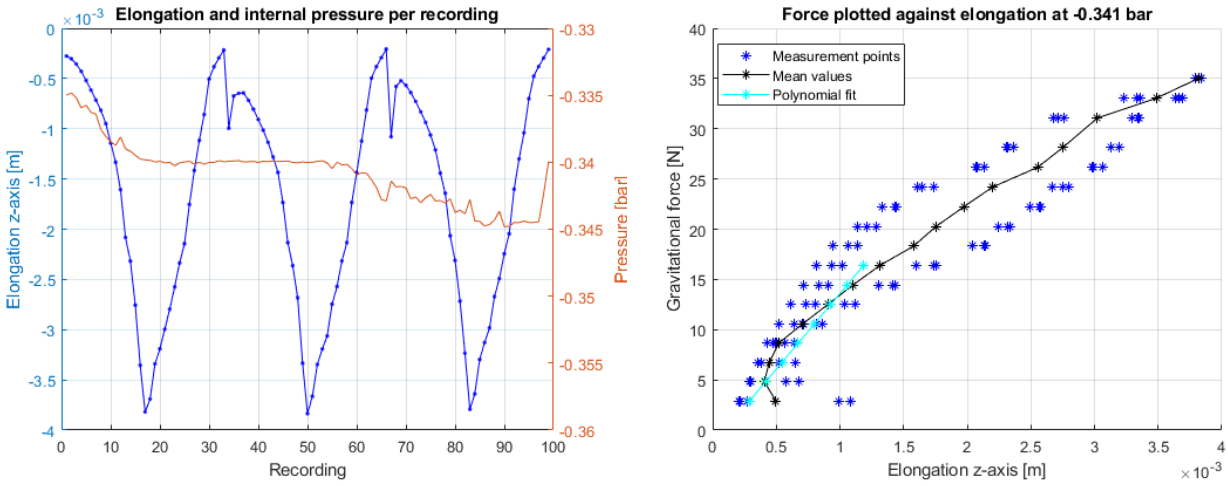

(a) (b)

Figure A.11: At -0.341 bar; (a) elongation and internal pressure plotted per recording; (b) elongation plotted against gravitational force.

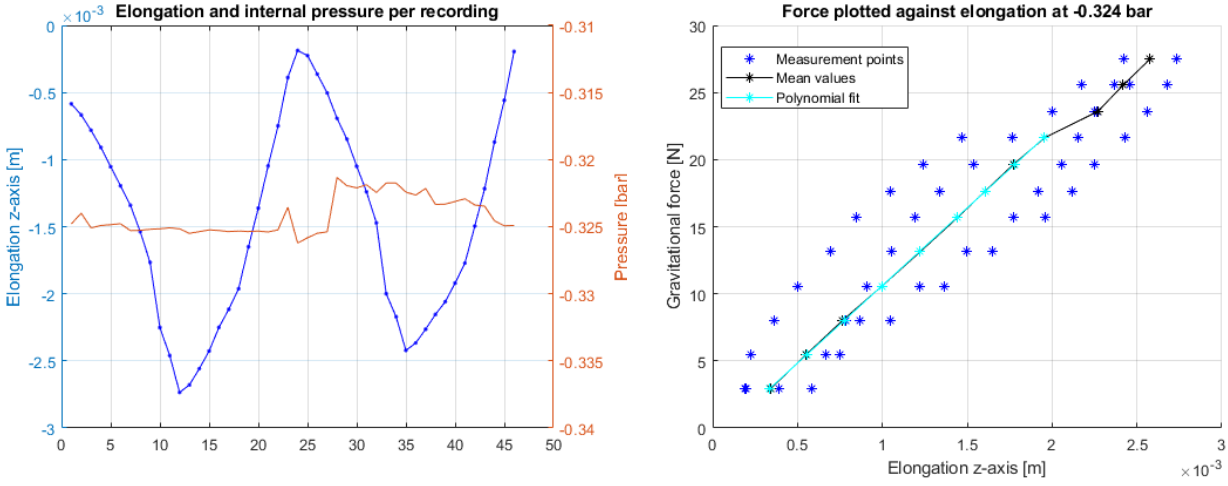

(a) (b)

Figure A.12: At -0.324 bar; (a) elongation and internal pressure plotted per recording; (b) elongation plotted against gravitational force.

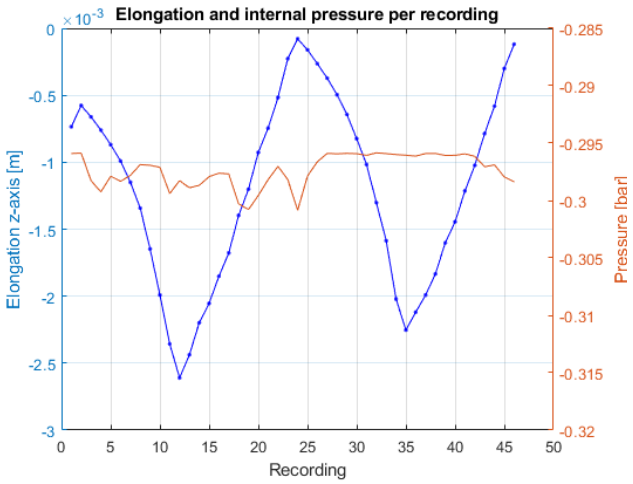

(a)

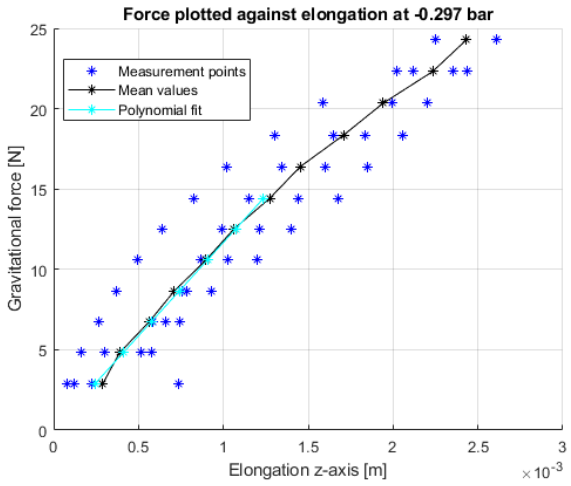

(b)

Figure A.13: At -0.297 bar; (a) elongation and internal pressure plotted per recording; (b) elongation plotted against gravitational force.

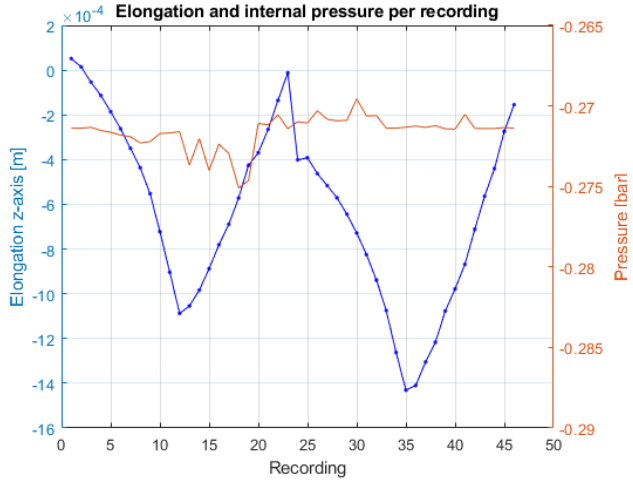

(a)

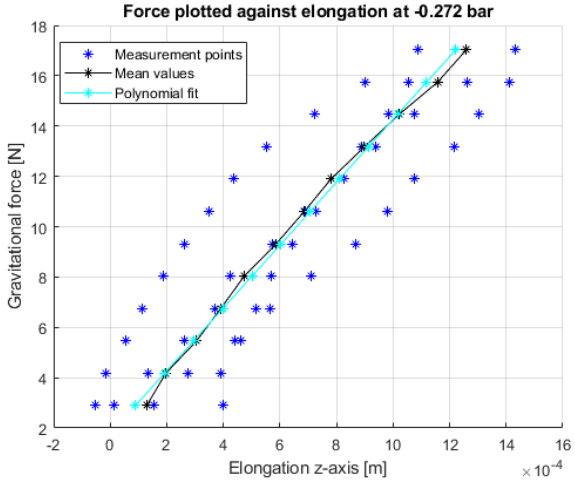

(b)

Figure A.14: At -0.272 bar; (a) elongation and internal pressure plotted per recording; (b) elongation plotted against gravitational force.

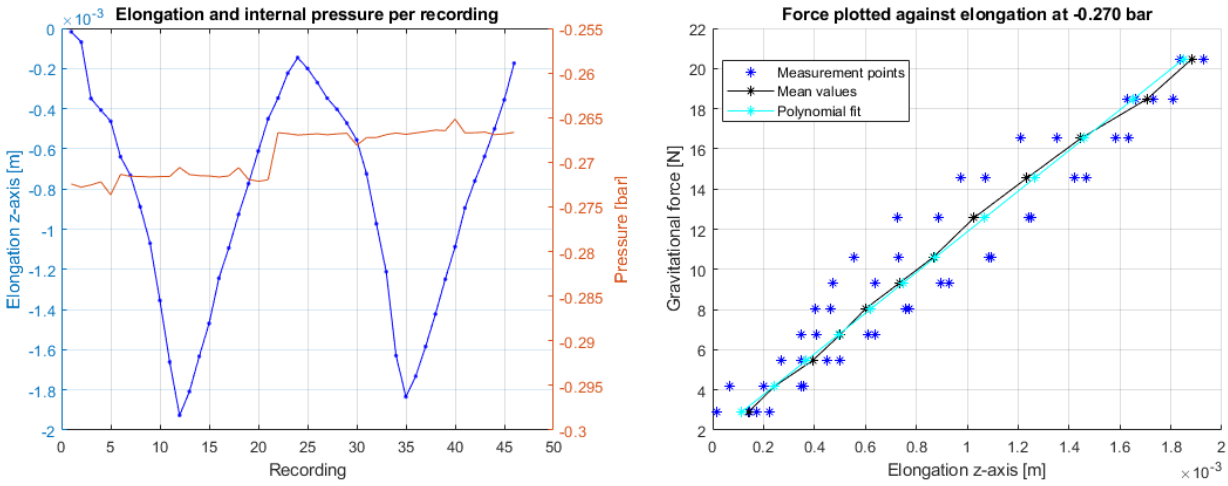

(a) (b)

Figure A.15: At -0.270 bar; (a) elongation and internal pressure plotted per recording; (b) elongation plotted against gravitational force.

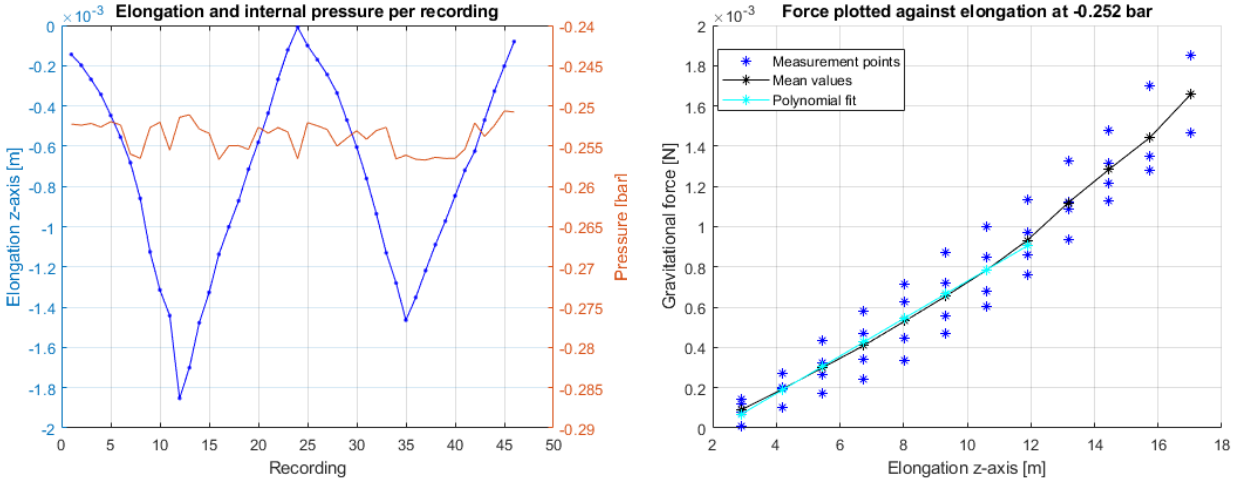

(a) (b)

Figure A.16: At -0.252 bar; (a) elongation and internal pressure plotted per recording; (b) elongation plotted against gravitational force.

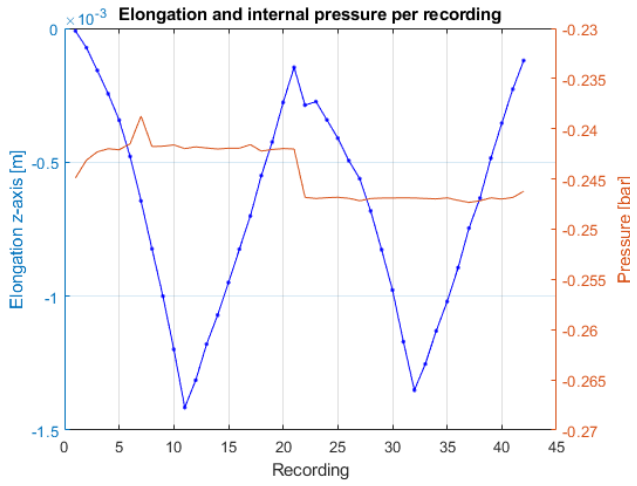

(a)

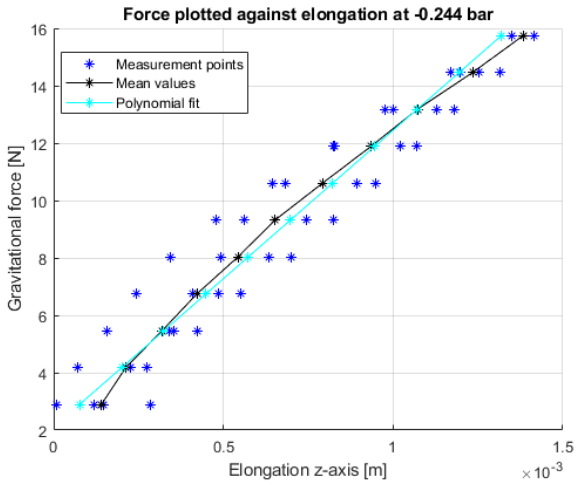

(b)

Figure A.17: At -0.244 bar; (a) elongation and internal pressure plotted per recording; (b) elongation plotted against gravitational force.

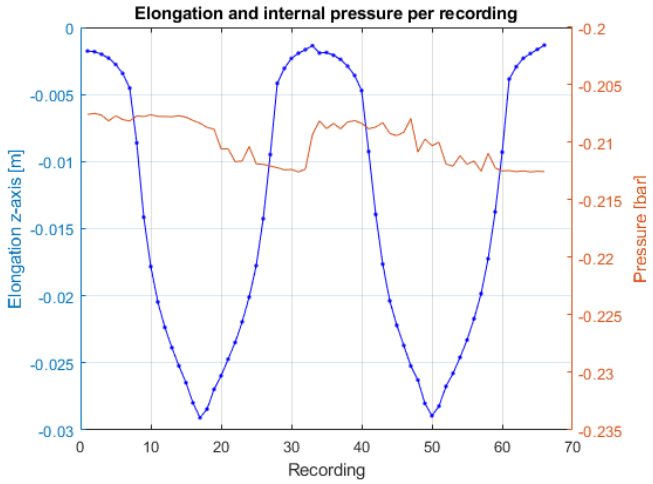

(a)

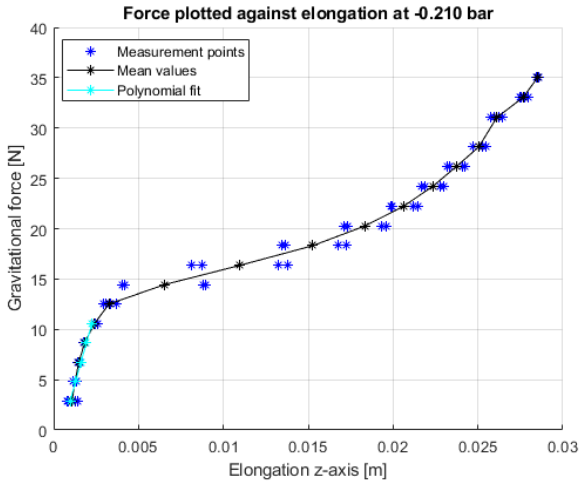

(b)

Figure A.18: At -0.201 bar; (a) elongation and internal pressure plotted per recording; (b) elongation plotted against gravitational force.

A.2 Validation measurement results

In this section the measurement results for the validation experiments are presented in similar plots. Experiments were done for a three different pressure levels for which a figure with the measured elongation and internal pressure are plotted per recording, plus a figure with the measured elongation plotted against gravitational force.

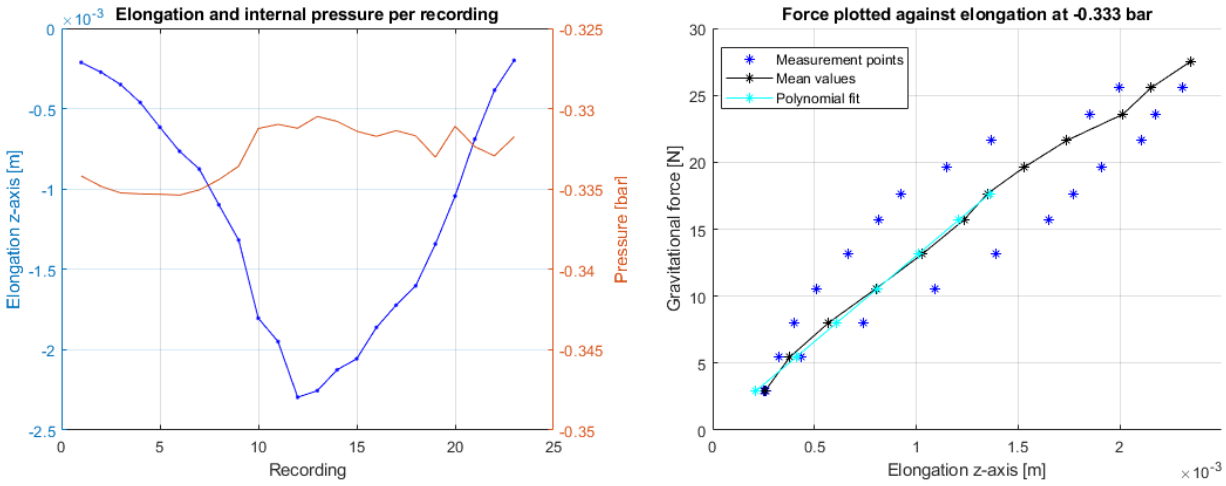

(a) (b)

Figure A.19: Validation at -0.333 bar; (a) elongation and internal pressure plotted per recording; (b) elongation plotted against gravitational force.

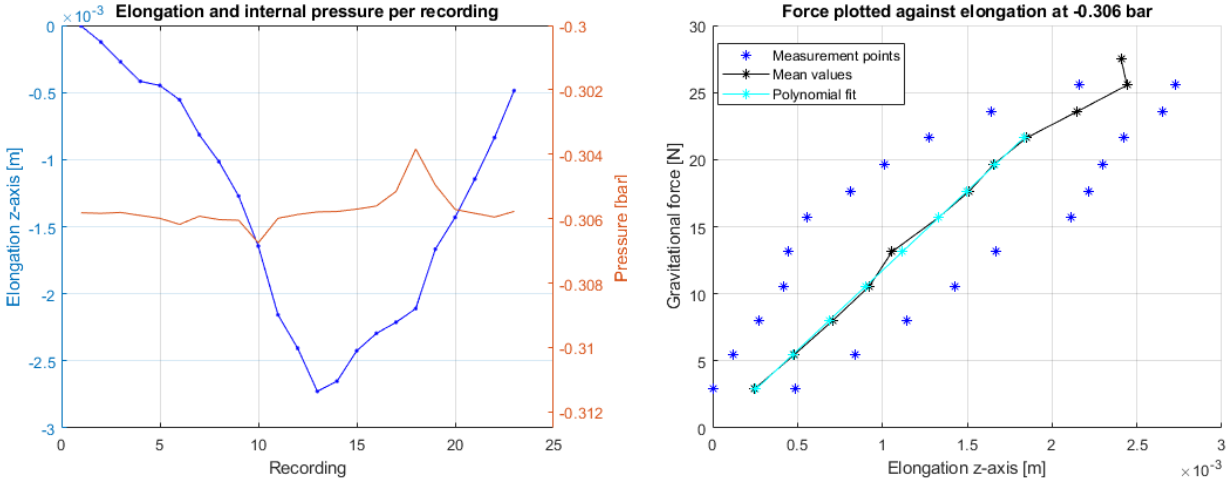

(a) (b)

Figure A.20: Validation at -0.306 bar; (a) elongation and internal pressure plotted per recording; (b) elongation plotted against gravitational force.

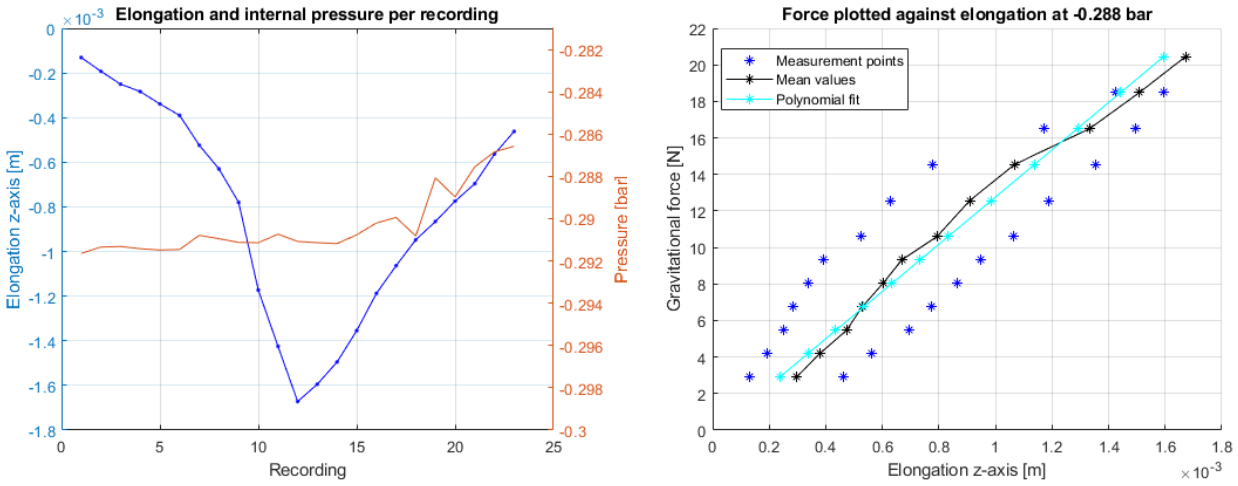

(a) (b)

Figure A.21: Validation at -0.288 bar; (a) elongation and internal pressure plotted per recording; (b) elongation plotted against gravitational force.

A.3 Total results

In this section, all the measurement results are collected into one table. This gives an overview of the linear stiffness and the maximum payload for each of the pressure levels for which experiments were conducted.

P_{inflow} [bar]	P_{sensor} [V]	$P_{internal}$ [bar]	Stiffness [N/m]	M_{max} [g]
	0.46	-0.396	32346	> 3500
4.0	0.4626	-0.394	30689	> 3500
	0.47	-0.387	29576	> 3500
3.6	0.4739	-0.384	28323	> 3500
	0.48	-0.378	27280	> 3500
	0.49	-0.369	25213	> 3500
3.3	0.4916	-0.368	23677	3500
	0.50	-0.360	20631	3500
	0.51	-0.351	17125	3200
	0.52	-0.342	15421	3200
3.0	0.5217	-0.341	15055	3000
	0.53	-0.333	13165	2900
	0.54	-0.324	12788	2900
	0.56	-0.306	10961	2800
	0.57	-0.297	10558	2700
	0.58	-0.288	10580	2700
2.5	0.5985	-0.272	10125	2700
	0.60	-0.270	10081	2700
	0.62	-0.252	9657.7	2500
2.3	0.6287	-0.244	9222.1	2500
2.0	0.667	-0.210	7873.4	2050

Table A.1: Per experiment: Inflow pressure, pressure sensor output, internal pressure of the suction cup, the derived linear stiffness and the maximum payload

TU/e EINDHOVEN UNIVERSITY OF TECHNOLOGY

Declaration concerning the TU/e Code of Scientific Conduct for the Bachelor's Final Project

I have read the TU/e Code of Scientific Conduct.
I hereby declare that my Bachelor's final project has been carried out in accordance with the rules of the TU/e Code of Scientific Conduct.

Date

17-01-2023

Name

Max Mage

ID-number

1246704

Signature

See:
The Netherlands Code of Conduct for Scientific Integrity, endorsed by 6 umbrella organizations, including the VSNU, can be found here also. More information about scientific integrity is published on the websites of TU/e and VSNU.